Title

ELECTRONIC TRANSITIONS IN SLOW COLLISIONS OF ATOMS AND MOLECULES. II. CALCULATION OF WAVE FUNCTIONS AND GREEN'S FUNCTIONS IN THE EIKONAL APPROXIMATION

Authors

Chen, Joseph C.Y.
Watson, Kenneth M.

Publication Date

1969-01-16

Submitted to The Physical Review

UCRL-18827
Preprint

cy. 2

ELECTRONIC TRANSITIONS IN SLOW COLLISIONS OF ATOMS AND MOLECULES. II. CALCULATION OF WAVE FUNCTIONS AND GREEN'S FUNCTIONS IN THE EIKONAL APPROXIMATION

Joseph C. Y. Chen and Kenneth M. Watson

January 16, 1969

AEC Contract No. W-7405-eng-48

LAWRENCE RADIATION LABORATORY
UNIVERSITY of CALIFORNIA BERKELEY

cy. 2

UCRL-18827

DISCLAIMER

UCRL-18827

ELECTRONIC TRANSITIONS IN SLOW COLLISIONS OF ATOMS AND MOLECULES. II. CALCULATIONS OF WAVE FUNCTIONS AND GREEN'S FUNCTIONS IN THE EIKONAL APPROXIMATION

Joseph C. Y. Chen*

Department of Physics and Institute for Pure and Applied Physical Sciences
University of California, San Diego, La Jolla, California

and

Kenneth M. Watson†

Department of Physics and Lawrence Radiation Laboratory
University of California, Berkeley, California

January 16, 1969

ABSTRACT

Practical techniques are developed for evaluating wave functions and Green's functions using the eikonal approximation. It is assumed that the scattering angle is small. This provides a great simplification in analysis of the trajectory curves, radii of curvature, etc. A sequence of approximations and the use of variational principles are described. Numerical illustrations, particularly for proton-hydrogen atom scattering, are given for several of the approximations.

---

* This research was supported in part by the Advanced Research Projects Agency of the Department of Defense and was monitored by the U.S. Army Research Office-Durham under Contract DA-31-124-ARO-D-257.

† This research was supported in part by the U.S. Atomic Energy Commission and the Air Force Office of Scientific Research.

IPAPS 68/69-280
January 1969

I. INTRODUCTION

In Part I of this series[1] we formulated a method for studying re-arrangement collisions between atoms (or molecules) using the eikonal approximation. The method was based on a form of the perturbed stationary state technique, using as basis function the adiabatic states (corrected for proper asymptotic boundary conditions). These basis states describe the elastic scattering of the two atoms (for simplicity, we shall refer to the colliding particles as atoms, even though one or both might be a molecule or ion) in the potential represented by the adiabatic molecular potential curve. The simplification of the theory which results from the use of the eikonal approximation for the adiabatic wave functions and Green's functions was discussed in I.

In this paper we discuss the actual construction of the distorted wave functions and Green's functions. Before beginning this, it is useful to review the range of certain parameters which will be of interest to us.

The reduced mass of the two colliding atoms is written as M and their relative coordinate $\underset{\sim}{R}$. The potential energy of interaction between them is taken to be $V(R)$.[2] The interaction $V(R)$ is assumed to have a range of order a_0, the Bohr radius; this is interpreted to mean that for R sufficiently greater than a_0 the potential is negligibly small. More precisely, we assume that

$$\lim_{(R/a_0) \to \infty} V(R) \leq \mathcal{O}(\text{constant}/R^{1+\delta}) , \tag{1.1}$$

where $\delta > 0$. For $R \leq a_0$, we characterize the strength of V as $|V(R)| \approx \mathcal{O}(\text{Ry})$ (here Ry = Rydberg) recognizing of course that V may be singular at $R = 0$.

The incident relative momentum of the colliding particles is $\underset{\sim}{p}$ and their center-of-mass energy is $\epsilon_p \equiv p^2/2M$. In atomic units this is $E \equiv \epsilon_p/Ry$. Our <u>first assumption</u> is that

$$E \gg 1 . \tag{1.2}$$

This implies the condition (II.3) that

$$\eta_3 \equiv \hbar/pa_0 = [920\, A_{eff}\, E]^{-1/2} \ll 1 . \tag{1.3}$$

Here we have introduced the notation

$$M/m \equiv 920\, A_{eff} , \tag{1.4}$$

where m is the mass of the electron.

Using the condition (1.2) we can write the classical scattering angle (in the center-of-mass corrdinate systems) for an impact parameter b as

$$\theta_c(b) = -\frac{b}{2E}\int_{-\infty}^{\infty} \frac{d}{dR_0}\left(\frac{V(R_0)}{Ry}\right)\frac{dz}{R_0} + \mathcal{O}(\theta_c^{\,2}) , \tag{1.5}$$

where $R_0 = [b^2 + z^2]^{1/2}$. Our second assumption, seen to be generally consistent with (1.2), is that

$$| \theta_c(b) | \ll 1 . \tag{1.6}$$

For order of magnitude estimates we shall assume that

$$| \theta_c | \approx \frac{1}{E} \tag{1.7}$$

for impact parameters of order a_0 .

In I the wave function describing the scattering was written in the form [Eqs. (I4.8) and (I4.35)]

$$\psi(\underset{\sim}{R}) = (2\pi)^{-3/2} A(\underset{\sim}{R}) e^{iS(\underset{\sim}{R})} , \tag{1.8a}$$

where $S(\underset{\sim}{R})$ is the eikonal,

$$S(\underset{\sim}{R}) = \int^{\underset{\sim}{R}} \kappa(\underset{\sim}{R}')ds , \tag{1.8b}$$

and

$$A(R) = \left(p/\kappa\right)^{1/2} \exp\left[- \frac{1}{2} \int^{\underset{\sim}{R}} \left(\frac{1}{\mathcal{R}_1} + \frac{1}{\mathcal{R}_2} \right) ds \right] . \tag{1.8c}$$

Here ds is an element of path length,

$$\kappa^2(R) = p^2 - 2 M V(R) \tag{1.9}$$

and the integrals are taken along the classical trajectory. The quantities $\mathcal{R}_1(\underset{\sim}{R})$ and $\mathcal{R}_2(\underset{\sim}{R})$ are the principal radii of curvature of the surface of constant eikonal which passes through $\underset{\sim}{R}$.

The functions[3] $\psi_{\underset{\sim}{p}}^{\pm}(\underset{\sim}{R})$ are obtained from Eqs. (1.8) by imposing the appropriate boundary conditions. This is illustrated in Fig. 1. For $\psi_{\underset{\sim}{p}}^{+}$ we have, when $\underset{\sim}{R}$ lies in the asymptotic region prior to scattering:

$$\underset{\sim}{\kappa}(\underset{\sim}{R}) = \underset{\sim}{p}$$

$$S_{\underset{\sim}{p}}^{+}(\underset{\sim}{R}) = \underset{\sim}{p}\cdot\underset{\sim}{R}$$

$$A(\underset{\sim}{R}) = 1 , \tag{1.10}$$

where $\underset{\sim}{\kappa}(\underset{\sim}{R})$ is the relative momentum vector at a point $\underset{\sim}{R}$ on the trajectory. For $\psi_{\underset{\sim}{k}}^{-}$ we have, when $\underset{\sim}{R}$ lies in the asymptotic post scattering region:

$$\underset{\sim}{\kappa}(\underset{\sim}{R}) = \underset{\sim}{k}$$

$$S_{\underset{\sim}{k}}^{-}(\underset{\sim}{R}) = \underset{\sim}{k}\cdot\underset{\sim}{R}$$

$$A(\underset{\sim}{R}) = 1 \; . \tag{1.11}$$

For the applications considered in this paper we may consider $k = p$.

The Green's function $\langle \underset{\sim}{R} \mid G \mid \underset{\sim}{R}' \rangle$ satisfies the same (Schrödinger) differential equation as $\psi^{\pm}(\underset{\sim}{R})$. Thus in the eikonal approximation [see Eq. (IV.25)]

$$\langle \underset{\sim}{R} \mid G \mid \underset{\sim}{R}' \rangle = A(\underset{\sim}{R}, \underset{\sim}{R}')\, e^{iS(\underset{\sim}{R},\underset{\sim}{R}')} \; , \tag{1.12}$$

where S and A are again given by Eqs. (1.8b) and (1.8c). The boundary condition imposed on G is [Eq. (I4.27)]

$$\lim_{\underset{\sim}{R} \to \underset{\sim}{R}'} \langle \underset{\sim}{R} | G | \underset{\sim}{R}' \rangle = -\frac{M}{2\pi} \, \frac{\exp[i\kappa(\underset{\sim}{R})\,|\underset{\sim}{R} - \underset{\sim}{R}'|]}{|\underset{\sim}{R} - \underset{\sim}{R}'|} \; . \tag{1.13}$$

The relative error resulting from the use of the eikonal approximation, Eqs. (1.8) or (1.12), is[4] of order

$$\eta(\text{eik}) \cong \left(\left| \frac{\hbar\theta_c}{pa_0} \right| \right) \approx [920\, A_{\text{eff}}\, E^3]^{-1/2} \; , \tag{1.14}$$

except for certain singular regions in the asymptotic domain [at $R \approx \mathcal{O}(a_0/|\theta_c|)$]. We see that, for particles of atomic mass,

$$\eta(\text{eik}) \ll 1 \tag{1.15}$$

whenever the condition (1.2) is satisfied. If we make the <u>further</u> approximation of setting $A(\underset{\sim}{R}) = 1$ in Eq. (1.8a) the relative error is of order

$$\eta_0(\text{eik}) \cong |\theta_c| \approx \frac{1}{E} , \tag{1.16}$$

except in certain asymptotic domains [this will be discussed in Sec. IV].

Making use of the condition (1.2) we shall obtain a series for S of the form:

$$S(R) = S_0 + S_1 + S_2 + \cdots , \tag{1.17}$$

where for $R \approx a_0$,

$$\begin{aligned} S_0 &= \mathcal{O}(p\, a_0) = \mathcal{O}([920\, A_{\text{eff}}\, E]^{1/2}) , \\ S_1 &= \mathcal{O}(p\, a_0\, |\theta_c|) = \mathcal{O}([920\, A_{\text{eff}}/E]^{1/2}) , \\ S_2 &= \mathcal{O}(p\, a_0\, \theta_c^{\,2}) = \mathcal{O}([920\, A_{\text{eff}}/E^3]^{1/2}) , \\ &\vdots \end{aligned} \tag{1.18}$$

We shall neglect terms of order S_3 and higher. That is, we shall take

$$S(\underset{\sim}{R}) = S_0 + S_1 + S_2 + \mathcal{O}(\eta_S) , \tag{1.19}$$

where

$$\eta_S \equiv p\, a_0\, |\theta_c|^3 \approx \left([920\, A_{\text{eff}}/E^5]^{1/2}\right) . \tag{1.20}$$

The approximation in which S_2 is neglected, so S is taken to be

$$S(\underset{\sim}{R}) \cong S_0 + S_1 \tag{1.21}$$

is called the "straight line" approximation. This approximation results on evaluating Eq. (1.8b) for a straight-line trajectory. The relative error in using (1.21) is of order

$$p\, a_0\, \theta_c^2 = \mathcal{O}\left([920\, A_{eff}/E^3]^{1/2}\right) . \tag{1.22}$$

The straight line trajectory approximation has long been used in quantum mechanics. It was given by Moliere in 1947[5] and applied to neutron scattering from nuclei by Fernbach, Serber, and Taylor.[6] Applications to the optical model of nuclear scattering were made by Francis and Watson[7] and by Glauber.[8]

Applications of the eikonal approximation to atomic scattering have been made by Bates and Holt,[9] by Smith and his collaborators.[10] An "eikonal-like" technique was recently proposed by Wilets and Wallace.[11]

Before closing this section, it may be well to emphasize that the criterion (1.14) for validity of the eikonal approximation by no means implies that the classical scattering amplitude is accurate. A somewhat crude estimate for the validity of the classical description of scattering may be obtained from the condition [a precise estimate was given in I and is given again in Eq. (5.19)]

$$|\theta_c| \gg \theta_{diff} , \tag{1.23}$$

where

$$\theta_{diff} \simeq \hbar/p\, a_0 \tag{1.24}$$

is the characteristic diffraction scattering angle from a potential of

range a_0 . From these expressions and Eqs. (1.3) and (1.7) we obtain the condition

$$\eta(\text{class}) \approx \left[\frac{E}{920\, A_{\text{eff}}}\right]^{1/2} \ll 1 , \tag{1.25}$$

if the scattering is to be classical. In Section V a more precise condition than (1.25) will be given.

II. GEOMETRICAL RELATIONS

In this section we discuss the classical trajectory in the center-of-mass system. This trajectory is specified by giving $\underset{\sim}{R}(t)$ as a function of t, having solved Newton's equations of motion:

$$\frac{d\underset{\sim}{\kappa}}{dt} = -\nabla V, \qquad \frac{d\underset{\sim}{R}}{dt} = M^{-1}\underset{\sim}{\kappa} . \tag{2.1}$$

We suppose $\underset{\sim}{R}(t)$ to lie in the $(\bar{x}, \bar{z})$ plane of a rectangular coordinate system, the plane being so positioned that $\underset{\sim}{R} = 0$ is at the origin and the trajectory is symmetric about the $\bar{x}$-axis. This is illustrated in Figs. (2a) and (2b), which refer respectively to the case of repulsive and attractive forces.

The condition (1.1) permits us to construct a circle "A" of radius A and with center at $\underset{\sim}{R} = 0$, so chosen that $V(R)$ may be neglected for $R > A$. Thus, outside "A" we may take the trajectory to be a straight line. In the asymptotic prior region outside "A", henceforth called region I, this line is parallel to the incident relative momentum $\underset{\sim}{p}$. In the asymptotic post region outside "A", called henceforth region II, the trajectory is parallel to a fixed vector $\underset{\sim}{p}_0$, obtained by rotating $\underset{\sim}{p}$ through an angle θ_c. [Note that θ_c is positive (negative) for an effectively repulsive (attractive) force, as obtained from Eq. (1.5).] At an arbitrary point on the trajectory, the local momentum vector is $\underset{\sim}{\kappa}$ and the local tangent is the unit vector $\hat{\underset{\sim}{\kappa}}$. Equations (2.1) of course imply that $\kappa(R)$ may be written as

$$\kappa(R) \equiv p[1 - U(R)] , \tag{2.2a}$$

where

$$U(R) \equiv 1 - [1 - V(R)/\epsilon_p]^{1/2}$$

$$= \frac{V}{2\epsilon_p} - \frac{1}{8}(V/\epsilon_p)^2 + \cdots . \qquad (2.2b)$$

It will be convenient to choose the coordinate $\bar{z}$ as the independent variable defining points on the trajectory (rather than the time t), so we shall write $\underset{\sim}{R} = \underset{\sim}{R}(\bar{z})$. The equation of the trajectory is then of the form

$$\bar{x}(\bar{z}) = d + h(\bar{z}) , \qquad (2.3a)$$

with

$$h(0) = 0 ,$$

$$h(-\bar{z}) = h(\bar{z}) . \qquad (2.3b)$$

Thus d is the <u>distance</u> of closest approach of the trajectory to the origin, as is illustrated in Figs. (2a) and (2b).

The angle between the tangent vector $\hat{\kappa}(\bar{z})$ and the $\bar{z}$ axis will be called $\beta(\bar{z})$. Thus,

$$\tan \beta(\bar{z}) = \frac{d\bar{x}}{d\bar{z}} . \qquad (2.4)$$

The asymptotic angle β is then

$$\beta = \lim_{\bar{z} \to \infty} \beta(\bar{z}) . \qquad (2.5)$$

Evidently,

$$\theta_c = 2\beta . \qquad (2.6)$$

In this coordinate system $S(\underset{\sim}{R}) = S(z,\rho)$, independent of the azimuthal angle ϕ [describing the orientation of the (z,x) plane]. Here we have written the radial coordinate as $\rho = |x|$.

In this new coordinate system the equation (2.14) for the trajectory becomes

$$x(\bar{z}) = [\bar{z} + |\bar{z}|] \sin\beta + b + \int_{|\bar{z}|}^{\infty} \Delta\beta(\bar{z}')\, d\bar{z}' + \mathcal{O}(|\beta^3|\, a_0) , \tag{2.16a}$$

and

$$z(\bar{z}) = \sec\beta[\bar{z}\cos^2\beta - |\bar{z}|\sin^2\beta] - b\tan\beta - \tan\beta \int_{|\bar{z}|}^{\infty} \Delta\beta(\bar{z}')d\bar{z}' + \mathcal{O}(\beta^4 a_0) . \tag{2.16b}$$

Finally, the radial distance $\rho(\bar{z},b)$ in a cylindrical coordinate system is

$$\rho(\bar{z}, b) = e(\bar{z})\, x(\bar{z}) ,$$

$$e(\bar{z}) \equiv x(\bar{z})/|x(\bar{z})| . \tag{2.16c}$$

To calculate the radii of curvature of $S(\underset{\sim}{R})$, we choose a fixed point $\underset{\sim}{R}_0$ and consider the surface passing through $\underset{\sim}{R}_0$:

$$S(\underset{\sim}{R}) = S(\underset{\sim}{R}_0) .$$

The normal to this surface at $\underset{\sim}{R}_0$ is the unit vector $\hat{\kappa}_0$, tangent to the trajectory passing through $\underset{\sim}{R}_0$ [this is illustrated in Fig. 4]. For a very small displacement $\hat{\kappa}_0 D$ from the point $\underset{\sim}{R}_0$, we have

$$S(\underset{\sim}{R}_0 + \hat{\kappa}_0 D) = S(\underset{\sim}{R}_0) + D\,\kappa(\underset{\sim}{R}_0) . \tag{2.17}$$

[This follows from the general theory of the eikonal:

$S(\underset{\sim}{R} + \underset{\sim}{\lambda}) = S(\underset{\sim}{R}) + \underset{\sim}{\lambda} \cdot \nabla S(\underset{\sim}{R})$ and $\nabla S(\underset{\sim}{R}) = \underset{\sim}{\kappa}(\underset{\sim}{R})$.]

We now introduce two orthogonal unit vectors, each perpendicular to $\hat{\kappa}_0$,

$$\hat{e}_1 = (1/\kappa)[S_z \hat{\rho} - S_\rho \hat{k}] ,$$

$$\hat{e}_2 = \hat{\phi} , \tag{2.18}$$

where

$$S_z = \left.\frac{\partial S(z,\rho)}{\partial z}\right|_\rho , \text{ etc.,}$$

and all quantities are evaluated at $\underset{\sim}{R}_0$. [Here $\hat{k}$, $\hat{\rho}$, $\hat{\phi}$ are the three basis vectors of the cylindrical coordinate system.]

A small displacement $\underset{\sim}{\lambda} = \lambda_1 \hat{e}_1 + \lambda_2 \hat{e}_2$ will represent a point on another constant eikonal surface defined by $S(\underset{\sim}{R}) = S(\underset{\sim}{R}_0 + \hat{\kappa}_0 D)$, where

$$D = \frac{1}{2}\left(\frac{\lambda_1^2}{\mathcal{R}_1} + \frac{\lambda_2^2}{\mathcal{R}_2}\right) . \tag{2.19}$$

Here $\mathcal{R}_1$ and $\mathcal{R}_2$ are the principal radii of curvature of the surface at $\underset{\sim}{R}_0$. This is illustrated in Fig. 5. We note that positive $\mathcal{R}_1$ ($\mathcal{R}_2$) corresponds to <u>convex</u> curvature as seen from a point <u>ahead</u> of $\underset{\sim}{R}_0$ on the trajectory.

Using Eqs. (2.17) and (2.19), we obtain

$$S(\underset{\sim}{R}_0 + \underset{\sim}{\lambda}) = S(\underset{\sim}{R}_0 + \hat{\kappa}_0 D)$$

$$= S(\underset{\sim}{R}_0) + \frac{\kappa}{2}\left(\frac{\lambda_1^2}{\mathcal{R}_1} + \frac{\lambda_2^2}{\mathcal{R}_2}\right) . \qquad (2.20)$$

By direct calculation using a Taylor expansion we obtain, on the other hand,

$$S(\underset{\sim}{R}_0 + \underset{\sim}{\lambda}) = S(\underset{\sim}{R}_0) + \frac{\lambda_2^2}{2\rho} S_\rho$$

$$+ \frac{\lambda_1^2}{2\kappa^2}\left[S_\rho^2 S_{zz} + S_z^2 S_{\rho\rho} - 2S_z S_\rho S_{z\rho}\right] . \qquad (2.21)$$

Thus,

$$\frac{1}{\mathcal{R}_1} = \frac{1}{\kappa^3}\left[S_\rho^2 S_{zz} - 2S_z S_\rho S_{z\rho} + S_z^2 S_{\rho\rho} \right] ,$$

$$\frac{1}{\mathcal{R}_2} = \frac{1}{\rho}\frac{S_\rho}{\kappa} . \qquad (2.22)$$

To lowest order in the small quantity $|\theta_c|$ we can considerably simplify these quantities. The angle which the tangent $\hat{\kappa}$ at a point $\bar{z}$ on a given trajectory makes with the z axis is

$$\theta_c(\bar{z},b) \equiv \beta + \beta(\bar{z}) , \qquad (2.23)$$

where we explicitly indicate the dependence on the impact parameter b, which of course acts as a trajectory label. Then

$$S_z = \kappa \cos\theta_c(z,b) \cong \kappa$$

and

$$S_\rho = \kappa \sin \theta_c(\bar{z},b) \cong \kappa\, \theta_c(\bar{z},b) .$$

This lets us write

$$\frac{1}{\mathcal{R}_2} \cong \frac{\theta_c(\bar{z},b)}{\rho} \tag{2.24}$$

and

$$\frac{1}{\mathcal{R}_1} \cong \frac{\partial\, \kappa\, \theta_c(\bar{z},b)}{\kappa\, \partial\, \rho}$$

$$\cong \frac{\partial\, \theta_c}{\partial\, b} \frac{\partial\, b}{\partial\, \rho} .$$

Now, to lowest order in θ_c, we obtain from Eq. (2.16a)

$$\frac{\partial\, b}{\partial\, \rho} = e(\bar{z}) \left[1 + \frac{1}{2} (\bar{z} + |\bar{z}|) \cos\beta \frac{d\, \theta_c(b)}{d\, b} \right]^{-1} ,$$

and thus

$$\frac{1}{\mathcal{R}_1} \cong e(\bar{z}) \frac{\partial\, \theta_c(\bar{z},b)}{\partial\, b} \left[1 + \frac{1}{2} (\bar{z} + |\bar{z}|) \cos\beta \frac{d\, \theta_c(b)}{d\, b} \right]^{-1} . \tag{2.25}$$

Here $\theta_c(b) = \lim_{\bar{z} \to \infty} \theta_c(\bar{z},b)$ is the scattering angle (1.5) and $e(\bar{z})$ is defined in Eq. (2.16c).

We now repeat the above calculation for the wave function $\psi_{\underset{\sim}{k}}^{-}$, as is illustrated in Fig. 3b. In this case Eqs. (2.15) are replaced by

$$z = \bar{z} \cos\beta + \bar{x} \sin\beta$$

$$x = -\bar{z} \sin\beta + \bar{x} \cos\beta . \tag{2.15ψ^-}$$

The trajectory equations (2.16) are replaced by

$$x(\bar{z}) = [\,|\bar{z}| - \bar{z}\,] \sin\beta + b + \int_{|\bar{z}|}^{\infty} \Delta\beta(\bar{z}')d\bar{z}' + \mathcal{O}(|\beta^3|\, a_0) ,$$

$$z(\bar{z}) = \sec\beta\, [\bar{z}\cos^2\beta + |\bar{z}|\sin^2\beta\,] + b\tan\beta$$

$$- \tan\beta \int_{|\bar{z}|}^{\infty} \Delta\beta(\bar{z}')d\bar{z}' + \mathcal{O}(|\beta^3|\, a_0) . \qquad (2.16\psi^-)$$

The angle of deflection (2.23) from $\hat{k}$ at any point $\bar{z}$ on the trajectory is now

$$\theta_c(\bar{z},b) = \beta - \beta(\bar{z}) . \qquad (2.23\psi^-)$$

Also, we now have $S_\rho \cong -\kappa\,\theta_c(\bar{z},b)$, so

$$\frac{1}{\mathcal{R}_2} \cong -\frac{\theta_c(\bar{z},b)}{\rho} . \qquad (2.24\psi^-)$$

Instead of Eq. (2.25) we have

$$\frac{1}{\mathcal{R}_1} \cong \frac{-\,e(\bar{z})\,[\partial\theta_c(\bar{z},b)]/\partial b}{\left[\,1 + \frac{1}{2}\,(|\bar{z}| - \bar{z})\cos\beta\,\frac{d\theta_c(b)}{db}\,\right]} . \qquad (2.25\psi^-)$$

III. CALCULATION OF THE EIKONAL

We are now ready to discuss the evaluation of the eikonal, as implied by Eq. (1.19). That is, we neglect terms of order

$$\eta_S = p\, a_0\, |\theta_c|^3 \approx [920\, A_{eff}/E^5]^{1/2} . \tag{3.1}$$

First, we calculate the eikonal for that part of the trajectory which lies inside the circle "A" of Figs. 2. Using Eqs. (1.8b), (2.1), and (2.12), this is

$$S_{12} = 2p \left\{ s(\bar{z}_2) - \int_0^{\bar{z}_2} U(\bar{R})\, \frac{ds}{d\bar{z}}\, d\bar{z} \right\} , \tag{3.2}$$

where

$$\bar{R} = [\, \bar{z}^2 + (d + h)^2 \,]^{1/2} \tag{3.3}$$

and $\bar{z}_2$ is as before the point at which the trajectory intersects the upper half of "A". Since we are neglecting terms of order η_S, we may set $ds/d\bar{z} = 1$ in the second term above. Thus, we have

$$S_{12} = 2p \left\{ \bar{z}_2 \sec\beta - \int_0^{\bar{z}_2} \left[\frac{1}{2} \left(\beta^2 - \beta^2(\bar{z}) \right) + U(\bar{R}) \right] d\bar{z} \right\} + \mathcal{O}(\eta_S)$$

$$= 2\, p \sec\beta\, \bar{z}_2 + \not{\phi}(b) + \mathcal{O}(\eta_S) , \tag{3.4}$$

where

$$\not{\phi}(b) \equiv - p \int_{-\infty}^{\infty} \left[\frac{1}{2} \left(\beta^2 - \beta^2(\bar{z}) \right) + U(\bar{R}) \right] d\bar{z} . \tag{3.5}$$

The quantity S_{12} may be put into the form of Eq. (1.19) by writing it as

$$S_{12} = 2p \left\{ \bar{z}_2 \sec\beta - \int_0^\infty U(R_0)\, d\bar{z}' \right.$$

$$\left. - \int_0^\infty \left[\frac{1}{2} (\beta^2 - \beta^2(\bar{z}')) + d \frac{dU}{dR_0} \frac{h}{R_0} \right] d\bar{z}' \right\}$$

$$+ \mathcal{O}(\eta_S) \qquad (3.6)$$

where R_0 is defined by Eq. (2.8).

We observe that when we evaluate S_{12} [or $S(\underset{\sim}{R})$ generally] to within the accuracy implied here, the angle $\beta(\bar{z})$ need be evaluated only to the lowest order that given by Eq. (2.7).

We also observe that according to the <u>principle of least action</u>[12] S_{12} is stationary with respect to a variation of trajectory about the exact trajectory. This means that we can use Eq. (3.6) to give a variational <u>principle</u> for obtaining $\beta(\bar{z})$. It also means that S_{12} is insensitive to the precise trajectory. [In Section VII we shall discuss the variational principle in more detail.]

We now calculate $S_{\underset{\sim}{p}}^{+}(\underset{\sim}{R})$, the eikonal for ψ_p^+ , to the same order. In the region I , prior to entering the circle "A" we have $S_{\underset{\sim}{p}}^{+} = \underset{\sim}{p}\cdot\underset{\sim}{R}$, as in Eq. (1.10). In all other domains we evidently have [recall that $\bar{z}_1 = -\bar{z}_2$]

$$S_{\underset{\sim}{p}}^{+}(\underset{\sim}{R}) = p \left\{ s(\bar{z}) - s(\bar{z}_1) - \int_{-\infty}^{\bar{z}} U(\bar{R})\, d\bar{z}' \right\} + \underset{\sim}{p}\cdot\underset{\sim}{R}_1 , \qquad (3.7)$$

where $\underset{\sim}{R}_1$ is the vector from the origin to the point at which the trajectory intersects "A" . Now, from Figs 2a , we see that

$$\underset{\sim}{p} \cdot \underset{\sim}{R}_1 = - p \bar{z}_2 \sec \beta - p b \tan \beta . \tag{3.8}$$

This lets us re-write Eq. (3.7) as [to order η_S]

$$S_{\underset{\sim}{p}}^{+}(\underset{\sim}{R}) = p s(\bar{z}) - p b \tan \beta - \frac{p}{2} \int_{-\infty}^{0} [\beta^2 - \beta^2(\bar{z})] d\bar{z} - p \int_{-\infty}^{z} U(R) d\bar{z}'$$

$$= p \bar{z} \sec \beta - p b \tan \beta + \phi(\bar{z}, b) , \tag{3.9}$$

where

$$\phi(\bar{z}, b) = - p \int_{-\infty}^{\bar{z}} \left[\frac{1}{2} \left(\beta^2 - \beta^2(\bar{z}') \right) + U(\bar{R}) \right] d\bar{z}' . \tag{3.10}$$

Equation (3.9) is valid over all $\underset{\sim}{R}$ space if we let the radius of "A" become infinite. In the asymptotic regime II, following the scattering we can write

$$S_{\underset{\sim}{p}}^{+}(\underset{\sim}{R}) = \underset{\sim}{p}_0 \cdot \underset{\sim}{R} - 2 p b \tan \beta + \phi(b) , \tag{3.11}$$

where $\phi(b)$ is given by Eq. (3.5). Here $\underset{\sim}{p}_0$ is the asymptotic final momentum, as in Fig. 2a.

The eikonal $S_{\underset{\sim}{k}}^{-}(\underset{\sim}{R})$ for the wave function $\psi_{\underset{\sim}{k}}^{-}$ is subject to the boundary condition (1.11). Referring to Fig. 2b and following the argument given above, we obtain to $\mathcal{O}(\eta_S)$

$$S_{\underset{\sim}{k}}^{-}(\underset{\sim}{R}) = k \bar{z} \sec \beta + k b \tan \beta + k \int_{z}^{\infty} \left[\frac{1}{2} \left(\beta^2 - \beta^2(\bar{z}') \right) + U(\bar{R}) \right] d\bar{z}' . \tag{3.12}$$

In the asymptotic region I ahead of the scattering this is

$$S_{\underset{\sim}{k}}^{-}(\underset{\sim}{R}) = \underset{\sim}{k}_{in}\cdot\underset{\sim}{R} + 2\,k\,b\tan\beta - \not{\phi}(b)\,, \tag{3.13}$$

since $\underset{\sim}{k}_{in}\cdot\underset{\sim}{R} = -k[|\bar{z}|\sec\beta + b\tan\beta]$ in region I .

In the "straight line" approximation we may drop the term S_2 in Eq. (1.19). In this case we may replace Eqs. (3.9) and (3.12) by

$$S_{\underset{\sim}{p}}^{+}(\underset{\sim}{R}) = p\,\bar{z}\sec\beta - p\,b\tan\beta - p\int_{-\infty}^{\bar{z}} U(R_0)d\bar{z}' + \mathcal{O}(\eta_{es})\,,$$

$$S_{\underset{\sim}{k}}^{-}(\underset{\sim}{R}) = k\,\bar{z}\sec\beta + k\,b\tan\beta + k\int_{\bar{z}}^{\infty} U(R_0)d\bar{z}' + \mathcal{O}(\eta_{es})\,, \tag{3.14}$$

where

$$\eta_{es} = p\,a_0\,|\theta_c|^2 \simeq [920\,A_{eff}/E^3]^{1/2}\,. \tag{3.15}$$

Again R_0 is defined by Eq. (2.8).

Also, in the "straight line" approximation we can write:

For $z < 0$, $\quad S_{\underset{\sim}{p}}^{+}(\underset{\sim}{R}) = \underset{\sim}{p}\cdot\underset{\sim}{R} - p\int_{-\infty}^{\bar{z}} U(R_0)d\bar{z}'\,,$

For $z > 0$, $\quad S_{\underset{\sim}{p}}^{+}(\underset{\sim}{R}) = \underset{\sim}{p}_0\cdot\underset{\sim}{R} - p\int_{-\infty}^{\bar{z}} U(R_0)d\bar{z}' - p\,b\,\theta_c\,,$

(Eq. 3.16 cont.)

$$\text{For } z > 0 , \qquad S_{\underset{\sim}{k}}^{-}(\underset{\approx}{R}) = \underset{\sim}{k}\cdot\underset{\approx}{R} + k\int_{\bar{k}}^{\infty} U(R_0)d\bar{z}' ,$$

$$\text{For } z < 0 , \qquad S_{\underset{\sim}{k}}^{-}(\underset{\approx}{R}) = \underset{\sim}{k}_{in}\cdot\underset{\approx}{R} + k\int_{\bar{k}}^{\infty} U(R_0)d\bar{z}' + p\, b\, \theta_c . \tag{3.16}$$

Note that our "straight line" approximation does not strictly correspond to a straight line. This is because $|\bar{z}\ p|$ may be arbitrarily large in the asymptotic domain.

IV. THE AMPLITUDE $A(\underset{\sim}{R})$

We consider first the amplitude (1.8c) for $\psi_{\underset{\sim}{p}}^{+}(\underset{\sim}{R})$ and evaluate this only to within relative order (θ_c^2).

For $x(\bar{z}) > 0$ we have from Eq. (2.16a)

$$\rho(\bar{z},\, b) \;=\; (\bar{z} + |\bar{z}|)\beta + b \;+\; \int_{|\bar{z}|}^{\infty} \Delta\beta(\bar{z}')\, d\bar{z}' + \mathcal{O}(\beta^2)\,. \tag{4.1}$$

If we hold b constant and vary $\bar{z}$, we obtain from this

$$\begin{aligned} d\rho(\bar{z},\, b) \;&=\; [\beta + \beta(\bar{z})]d\bar{z} \\ &=\; \theta_c(\bar{z},\, b)d\bar{z}\,, \end{aligned} \tag{4.2}$$

according to Eq. (2.23). Thus, using Eq. (2.24) we find

$$\int_{-\infty}^{\bar{z}} \frac{d\bar{z}'}{\mathcal{R}_2} \;=\; \int_{-\infty}^{\bar{z}} \frac{d\rho}{\rho} \;=\; \ell n\big(\rho(\bar{z},\, b)/b\big)\,. \tag{4.3}$$

Also, using Eq. (2.25) we obtain

$$\begin{aligned} \int_{-\infty}^{\bar{z}} \frac{d\bar{z}'}{\mathcal{R}_1} \;&=\; \int_{-\infty}^{\bar{z}} d\;\ell n\left(\frac{\partial\rho}{\partial b}\right) \\ &=\; \ell n\left[\left(\frac{\partial\rho(\bar{z},\, b)}{\partial\, b}\right)\left(\frac{\partial\rho(-\infty,\, b)}{\partial\, b}\right)^{-1}\right] \\ &=\; \ell n\left[\frac{\partial\rho(\bar{z},\, b)}{\partial\, b}\right]\,. \end{aligned} \tag{4.4}$$

Substitution of these results into Eq. (1.8c) now gives us

$$A(\underset{\sim}{R}) = \left[(1 - U) \left(\frac{\rho}{b} \frac{\partial \rho}{\partial b} \right) \right]^{-1/2} , \qquad (4.5)$$

which is just the exact expression (I 4.9). Equation (4.5) may be evaluated using Eq. (4.1).

We note that $A(\underset{\sim}{R})$ is singular in the asymptotic post region II for

$$\bar{z}\, \theta_c(b) = -b , \qquad \theta_c(b) < 0 \qquad (4.6a)$$

and for

$$\bar{z}\, \frac{d\theta_c(b)}{db} = -1 , \qquad \frac{d\theta_c(b)}{db} < 0 . \qquad (4.6b)$$

These singularities are suggestive of the familiar Stokes phenomenon occurring in the WKB solution. The eikonal approximation (1.8) breaks down at either of these singularities. To integrate past these, more elaborate methods than those given here are required. Fortunately, for the applications which we have in mind, the wave functions $\psi_{\underset{\sim}{p}}^{\pm}$ are not required in the far asymptotic region implied by Eqs. (4.6).

It is evident from Eq. (4.1) that Eq. (4.5) does not approach its correct asymptotic form when either $\beta = 0$ or $d\beta/db = 0$. This can be seen by writing $A(\underset{\sim}{R})$ in the approximate form, valid for large $\bar{z}$,

$$A(\underset{\sim}{R}) \cong \left(1 + \frac{U}{2}\right) \left[\left(1 + \frac{\bar{z} + |\bar{z}|}{2} \frac{\theta_c(b)}{b} \right) \left(1 + \frac{\bar{z} + |\bar{z}|}{2} \frac{d\theta_c}{db} \right) \right]^{-1/2} .$$

The case that $\theta_c(b) = 0$ is called a "glory", while $d\theta_c/db = 0$ gives "rainbow" scattering. Ford and Wheeler[13] have shown that the

classical description of scattering fails in either of these cases. This is clear from the above expression, since then $A(\underset{\sim}{R})$, does not approach its correct asymptotic form. Equation (5.11) of the next section may be used to describe scattering at angles near either a rainbow or a glory. The result is of course equivalent to that of Ford and Wheeler.[13]

To obtain the amplitude factor $A(\underset{\sim}{R})$ for $\psi_{\underset{\sim}{k}}^{-}$, we first use the first of Eqs. (2.15ψ^{-}) to write, for $x(\bar{z}) > 0$

$$\rho(\bar{z}, b) = (|\bar{z}| - \bar{z})\beta + b + \int_{|\bar{z}|}^{\infty} \Delta\beta(\bar{z}')\, d\bar{z}' + \mathcal{O}(\beta^2) . \qquad (4.1\psi^{-})$$

The expression (4.5) remains valid, but is now to be evaluated using Eq. (4.1ψ^{-}).

V. THE ELASTIC SCATTERING AMPLITUDE

Using the eikonal wave function (1.8) we may write the T matrix for scattering from an asymptotic momentum $\underset{\sim}{p}$ into an asymptotic momentum $\underset{\sim}{k}$ as

$$T = (2\pi)^{-3/2} \int d^3R \; e^{-i\underset{\sim}{k}\cdot\underset{\sim}{R}} \; V(R) \; \psi_{\underset{\sim}{p}}^{+}(\underset{\sim}{R})$$

$$= (2\pi)^{-3} \int d^3R \; V(R) \; A(R) \exp\left\{ i[S_{\underset{\sim}{p}}^{+}(\underset{\sim}{R}) - \underset{\sim}{k}\cdot\underset{\sim}{R}] \right\} , \tag{5.1}$$

where in the second writing the relative error is of order $\eta(eik)$, Eq. (1.14). We showed in I that the classical amplitude is obtained from (5.1) when condition (1.25) is met. In this case, of course, we have $\theta = |\theta_c|$, where θ is the scattering angle defined by

$$\cos\theta = \hat{k} \cdot \hat{p} \; .$$

In addition to the assumed condition (1.6) that $|\theta_c| \ll 1$, we shall also suppose that

$$\theta \ll 1 \; .$$

Finally, we continue to assume that the expression (1.19) for $S_{\underset{\sim}{p}}^{+}$ is valid, quantities of order

$$\eta_S \equiv p \, a_0 \, |\theta_c|^3$$

being negligible. We shall also consider $\eta_\theta \equiv p \, a_0 \, \theta^3$ to be negligible.

We see from Eq. (4.5) and (4.1) that to relative order $|\theta_c|$, we may set

$$A(\underset{\sim}{R}) = 1$$

in Eq. (5.1). We have then to evaluate

$$T = (2\pi)^{-3} \int d^3R \; V(R) \exp[i \, S_{\underset{\sim}{p}}^{+}(\underset{\sim}{R}) - \underset{\sim}{k}\cdot\underset{\sim}{R}] \; . \tag{5.2}$$

We now shall use a cylindrical coordinate system, with variables (z, ρ, ϕ) to carry out the integration above. Then

$$d^3R = \rho \, d\rho \, d\phi \, dz \; . \tag{5.3}$$

In this coordinate system we may re-write Eq. (3.9), using Eq. (2.15b), as

$$\text{for } \bar{z} > 0 \, , \qquad S_{\underset{\sim}{p}}^{+}(\underset{\sim}{R}) = p \, z \sec\theta_c + p \, \beta \int_{|\bar{z}|}^{\infty} \Delta\beta(\bar{z}') \, d\bar{z}'$$

$$+ \mathcal{J}(\bar{z}, b) + \mathcal{O}(\eta_S) \, , \tag{5.4a}$$

and

$$\text{for } \bar{z} < 0 \, , \qquad S_{\underset{\sim}{p}}^{+}(\underset{\sim}{R}) = p \, z + p \, \beta \int_{|\bar{z}|}^{\infty} \Delta\beta(\bar{z}') \, d\bar{z}'$$

$$+ \mathcal{J}(z, b) + \mathcal{O}(\eta_S) \, . \tag{5.4b}$$

Also, using Eq. (2.16a) with $\rho = x(\bar{z})$,

$$\underset{\sim}{k}\cdot\underset{\sim}{R} = p\, z \cos\theta + p\, \rho \sin\theta \cos\phi$$

$$= p\, z \cos\theta + p \sin\theta \cos\phi \left[(\bar{z} + |\bar{z}|) \sin\beta + b + \int_{|\bar{z}|}^{\infty} \Delta\beta\, d\bar{z}' \right].$$

This lets us write, to relative order η_S, η_θ, etc.,

for $\bar{z} > 0$,

$$S_{\underset{\sim}{p}}^{+} - \underset{\sim}{k}\cdot\underset{\sim}{R} = p\, z \sec\theta_c \,[1 - \hat{p}_0\cdot\hat{k}\,] + p \int_{|\bar{z}|}^{\infty} \Delta\beta\, d\bar{z}'[\sin\beta - \sin\theta\cos\phi] - p\, b \sin\theta\cos\phi + \bar{\phi}(\bar{z}, b), \tag{5.5a}$$

and

for $\bar{z} < 0$,

$$S_{\underset{\sim}{p}}^{+} - \underset{\sim}{k}\cdot\underset{\sim}{R} = p\, z[1 - \cos\theta] + p \int_{|\bar{z}|}^{\infty} \Delta\beta\, d\bar{z}'[\sin\beta - \sin\theta\cos\phi] - p\, b \sin\theta\cos\phi + \bar{\phi}(\bar{z}, b). \tag{5.5b}$$

Now, we saw in I that in the classical limit the important contribution to the integral in (5.2) comes from $\bar{z}$ in the near asymptotic post scattering region. This means that in the classical limit we can set

$$\int_{\bar{z}}^{\infty} \Delta\beta \, d\bar{z}' = \mathcal{O}(\beta^2) .$$

Also, in the classical limit $\hat{\underset{\sim}{p}}_0 \cdot \hat{\underset{\sim}{k}} = 0$. Therefore in the classical limit we have

$$S_{\underset{\sim}{p}}^{+} - \underset{\sim}{k}\cdot\underset{\sim}{R} = \bar{\phi}(\bar{z}, b) - p\, b \sin\theta \cos\phi , \tag{5.6}$$

to within the order η_S, η_θ, etc.

The classical limit fails, as we have seen, when

$$|\theta_c| \, p \, a_0 \lesssim 1 . \tag{5.7}$$

Thus, when the classical limit is <u>not</u>, valid, we have $\theta_c^2 \, p \, a_0 \ll 1$, $\theta^2 \, p \, a_0 \ll 1$, $\theta \, |\theta_c| \, p \, a_0 \ll 1$. In this case we again see that Eq. (5.6) may be used. In any case, we may now write Eq. (5.2) as

$$\begin{aligned} T &= (2\pi)^{-3} \int \rho \, d\rho \, dz \, d\phi \, V(R) \exp\{-i\, p\, b \sin\theta \cos\phi\} \, e^{i\bar{\phi}} \\ &= (2\pi)^{-2} \int \rho \, d\rho \, dz \, V(R) \, J_0(p\, b \sin\theta) \, e^{i\bar{\phi}(\bar{z},b)} . \end{aligned} \tag{5.8}$$

To relative order $|\theta_c|$ we have

$$\rho \, d\rho \, dz = b \, db \, d\bar{z} , \tag{5.9}$$

and, to the same relative order,

$$V(R) d\bar{z} = - v \, d\bar{\phi} , \tag{5.10}$$

where $v \equiv p/M$ is the asymptotic relative velocity. This lets us write

$$T = -\frac{v}{i(2\pi)^2} \int_0^\infty b\, db\, J_0(p\, b\, \theta)[e^{i\bar{\phi}(b)} - 1] , \tag{5.11}$$

where

$$\bar{\phi}(b) = \lim_{\bar{z} \to +\infty} \phi(\bar{z}, b) \tag{5.12}$$

is defined by Eq. (3.5).

Equation (5.11) would reduce to the familiar expression of Moliere[5] if we were to drop the term S_2 in Eq. (1.19). The increased generality in the quantity $\bar{\phi}(b)$ has not, therefore, altered the simple form of (5.11).

It is instructive to retrieve the classical limit from Eq. (5.11). To do this, we introduce the classical scattering angle θ_c, defined to accuracy of $\bar{\phi}$,

$$p\, \theta_c(b) \equiv \frac{\partial \bar{\phi}(b)}{\partial b} ,$$

$$\theta_c'(b) \equiv \frac{\partial \theta_c}{\partial b} , \cdots , \tag{5.13}$$

and

$$e_1 \equiv \theta_c(b)/|\theta_c(b)| . \tag{5.14}$$

Then, on using the asymptotic form for the Bessel function, we have

$$T \cong -\frac{v}{2i(2\pi)^2} \left[2/\pi\theta p\right]^{1/2} \int_0^\infty b^{1/2}\, db\, e^{i\gamma(b)}\, e^{ie_1\frac{\pi}{4}} , \tag{5.15}$$

where

$$\gamma(b) \equiv \mathcal{J}(b) - e_1 \, p \, b \, \theta \, . \tag{5.16}$$

Now, the stationary phase point at $b = b_c$ is obtained from

$$\frac{\partial \gamma}{\partial b_c} = p\left(-\theta_c(b_c) + e_1 \, \theta\right) = 0 \, ,$$

or

$$\theta = |\theta_c(b_c)| \tag{5.17}$$

defines b_c . This lets us write in the integrand of Eq. (5.15),

$$\gamma(b) = \gamma(b_c) + \frac{p}{2} \frac{\partial \theta_c}{\partial b_c} (b - b_c)^2 + \mathcal{O}\left(\eta(\text{class})\right) , \tag{5.18}$$

where

$$\eta(\text{class}) = \left| \frac{\partial^2 \theta_c}{\partial b^2} \right| \left[p^{1/2} \left| \frac{\partial \theta_c}{\partial b} \right|^{3/2} \right]^{-1} . \tag{5.19}$$

[This provides a more precise definition than that given by Eq. (1.25).]

A stationary phase evaluation of Eq. (5.15) now leads directly to the

<u>classical scattering matrix</u>

$$T \cong -[(2\pi)^2 M]^{-1} \left[\frac{b_c}{\theta} \left| \frac{db_c}{d\theta} \right| \right]^{1/2} \exp\left[i\left(\mathcal{J}(b_c) - e_1 \, p \, b_c \, \theta\right)\right]$$
$$\times \exp\left[i \frac{\pi}{4} \left(e_1 + \frac{\partial \theta_c}{\partial b_c} \left[\left| \frac{\partial \theta_c}{\partial b_c} \right| \right]^{-1} - 2 \right) \right] . \tag{5.20}$$

Finally, we see from Eqs. (3.10) and (1.5) that

$$\Theta_c(b) = \theta_c(b) + \mathcal{O}(\theta_c^2) . \qquad (5.21)$$

Thus, $\Theta_c = \theta_c$ to within the accuracy with which we have calculated the classical scattering.

A familiar expression for the total scattering cross section may be obtained from Eq. (5.11). We have

$$\sigma \cong 2\pi \int \sin\theta \, d\theta \, (2\pi)^4 M^2 \, |T|^2 . \qquad (5.22)$$

Now, if we write

$$\int_0^\pi \sin\theta \, d\theta \, J_0(p\, b\, \theta) \, J_0(p\, b'\, \theta) \cong \frac{1}{p^2} [\delta(b - b')]/b , \qquad (5.23)$$

we obtain

$$\sigma = 8\pi \int b \, db \, \sin^2 \left(\Phi(b)/2\right) . \qquad (5.24)$$

VI. THE GREEN'S FUNCTION

The Green's function $\langle \underset{\sim}{R} |G| \underset{\sim}{R}' \rangle$ was given in the eikonal approximation by Eq. (1.12). The eikonal in this case is

$$S(\underset{\sim}{R}, \underset{\sim}{R}') = \int_{\underset{\sim}{R}'}^{\underset{\sim}{R}} \kappa(\bar{R})\, ds , \tag{6.1}$$

where the integral is taken from a point $\underset{\sim}{R}'$ to a point $\underset{\sim}{R}$ along the trajectory linking these two points. We may evidently so rotate our $(\bar{z}, \bar{x})$ coordinate axes that Figs. 2 apply. We may then use Eq. (3.9), writing

$$S(\underset{\sim}{R}, \underset{\sim}{R}') = S_{\underset{\sim}{p}}^{+}(\underset{\sim}{R}) - S_{\underset{\sim}{p}}^{+}(\underset{\sim}{R}') , \tag{6.2}$$

where $\underset{\sim}{p}$ and the impact parameter are chosen to ensure that the trajectory pass through both $\underset{\sim}{R}$ and $\underset{\sim}{R}'$.

The principle of least action may be used as a variational principle to calculate $S(\underset{\sim}{R}, \underset{\sim}{R}')$. That is, $S(\underset{\sim}{R}, \underset{\sim}{R}')$ is stationary if we hold $\underset{\sim}{R}$ and $\underset{\sim}{R}'$ fixed and make small variations in the trajectory.

For our applications to atomic reactions the points $\underset{\sim}{R}$ and $\underset{\sim}{R}'$ will ordinarily both lie within the range of strong interaction. This means that we can, for most applications, approximate $A(\underset{\sim}{R}, \underset{\sim}{R}')$ in Eq. (1.12) as

$$A(\underset{\sim}{R}, \underset{\sim}{R}') \cong -\frac{M}{2\pi} \left(|\underset{\sim}{R} - \underset{\sim}{R}'| \right)^{-1} . \tag{6.3}$$

The principal radii of curvature may then be approximately written as

$$\mathcal{R}_1 \cong \mathcal{R}_2 \cong |\underset{\sim}{R} - \underset{\sim}{R}'| \ . \qquad (6.4)$$

The relative error in both cases above is of $\mathcal{O}(|e_c|)$.

VII. APPROXIMATION METHODS

We have already noted that according to the principle of least action the quantity S_{12} [Eq. (3.2)] is stationary if we hold the end points fixed and vary the trajectory about its correct value. This suggests that the eikonal is somewhat insensitive to the actual trajectory chosen. It also means that we can use (3.2) to provide a variational principle for calculating the trajectory.

The simplest generalization of the straight line trajectory is that consisting of two straight line segments intersecting at an angle 2β, as is illustrated in Fig. 6. [If we consider β to be a variational parameter, and vary β to minimize S_{12}, we of course obtain $2\beta = \theta_c$, as given by Eq. (1.5).] In this case, which we call the "angle" approximation, Eq. (2.13b) reduced to

$$b = d \cos \beta , \tag{7.1}$$

and Eq. (2.12) becomes

$$s(\bar{z}) = \bar{z} \sec \beta . \tag{7.2}$$

The expression (3.10) simplifies to the form

$$\begin{aligned} \mathcal{J}(\bar{z}, b) &= - p \int_{-\infty}^{\bar{z}(-)} U(R_1) d\zeta , \qquad \bar{z} < 0 \\ &= - p \int_{-\infty}^{\bar{z}(+)} U(R_1) d\zeta + 2 p U(d) d \sin \beta , \qquad \bar{z} > 0 , \end{aligned} \tag{7.3}$$

where $\bar{z}(\pm) \equiv \bar{z} \sec \beta \pm d \sin \beta$ and $R_1^2 = b^2 + \zeta^2$. In obtaining Eq. (7.3) we have set

$$\int_0^{d \sin \beta} U(R_1) d\zeta \cong U(d)\, d \sin \beta ,$$

etc. The phase (5.12) appearing in the T matrix is obtained from (7.3) as

$$\delta(b) = - p \int_{-\infty}^{\infty} U(R_1) d\zeta + 2 p \beta d\, U(d) + \mathcal{O}(p\, a_0 |\beta|^3) . \qquad (7.4)$$

The "angle" approximation thus differs from the "straight line" approximation only by the addition of the term $2 p \beta U(d)$.

We mention that when it is possible to write $U(R)$ in the form

$$U(R) = \sum_{s=1}^{P} a_s / R^s , \qquad (7.5)$$

with the a_s constant, the integrals (7.4) and (2.7) can be done analytically. Also, if we write

$$\beta(\bar{z}) = c_0 + \sum_{s=2}^{Q} c_s / R^s , \qquad (7.6)$$

the integrals (2.11) and (2.12) can be done analytically. In this case the coefficients $c_0, \cdots c_Q$ may be treated as variational parameters in S_{12} .

To provide a simple numerical comparison of the "straight line" and "angle" approximations with the "exact" expression (3.5) for $\delta(b)$, we write

$$U(R) = D/R^2 . \qquad (7.7)$$

The expression for β, as obtained from Eqs. (2.5) and (2.7), is

$$\beta = \frac{\pi}{2} \frac{D}{b^2} \quad . \tag{7.8}$$

The corresponding expressions for $\not\phi$ in the "straight line" and "angle" approximations are then[14]

$$\begin{aligned} \not\phi(b) &= -2\,p\,b\,\beta \quad \text{(straight line)} \\ &= -2\,p\,b\,\beta\left(1 - \frac{2}{\pi}\beta\right) \quad \text{(angle).} \end{aligned} \tag{7.9}$$

In Fig. 7 we show the resulting values of $\not\phi$ given as a function of $\theta_c = 2\beta$. In this calculation we chose $D = 0.025$ and $p = 136$ (both in atomic units). We have given $\not\phi$ here for β extending over the range $0 < \beta < 1$. The "exact" expression is of course no longer exact for $\beta \approx 1$ since we have replaced $\cos\beta$ by $1 - \frac{1}{2}\beta^2$ in Eq. (3.5) and $\tan\beta$ by β in Eq. (2.9) for h. The results of Fig. 7 do suggest, however, that the "angle" approximation, which represents an almost trivial generalization of the "straight line" approximation, can be considerably more accurate than the latter.

VIII. APPLICATION TO THE (H^+, H) SYSTEM

As a first application of the approximate methods developed in the previous sections to physical processes in an actual collision system, we consider the elastic scattering and resonant electron-transfer processes in the (H^+, H) collision system. Since the adiabatic potentials for this system are known accurately,[15] we are in a position to evaluate directly the validity of the various approximations without ambiguities resulting from uncertainties in the potentials.

The (H^+, H) collision system is a system having symmetries with respect to the interchange of the protons and upon reflection of the electron coordinates in the internuclear plane. As a consequence, we have the "gerade" and "ungerade" symmetries for the electronic states and a parity restriction for the angular momentum states of the nuclear motion. For a given electronic state the angular momentum quantum number L for the motion of the protons is limited either to even or odd values. We have the symmetry properties for the scattering amplitude $f(\theta)$

$$\begin{aligned} f(\theta) &= f(\pi - \theta), \qquad L \text{ even} \\ f(\theta) &= -f(\pi - \theta), \qquad L \text{ odd}. \end{aligned} \tag{8.1}$$

This would give rise to oscillations in the differential cross sections resulting from the interference between $f(\theta)$ and $f(\pi - \theta)$.[16,17] Such interference would become appreciable only at large L and large scattering angles. For the present interest in small angle scattering [see Eqs. (1.6)

and (1.7)] we neglect for the moment such interference.

The "gerade" and "ungerade" symmetry of the electronic states which give rise to separate potential energies of interaction between H^+ and H must explicitly be considered. In dealing with the elastic scattering and resonant electron-transfer processes between H^+ and H, we assume that the interaction potential is given by the $^2\Sigma_g^+ H_2^+$ (gerade) and the $^2\Sigma_u^+ H_2^+$ (ungerade) adiabatic potentials. This assumption neglects any coupling of the elastic-scattering and electron-transfer channels with the collisional excitation, electron-transfer excitation and ionization channels. This would be a reasonable assumption if the condition for the near-adiabatic scattering $\eta_2 \ll 1$ [Eq. (11.2)] is satisfied and if there is no near crossings of the adiabatic states. For the (H^+, H) system such an assumption, is, however, an oversimplification since in the united atom limit the $2p\sigma$ and $2p\pi$ states of H_2^+ are degenerate and therefore strongly coupled. This oversimplification nevertheless should not affect our study of the trajectory problem.

In this approximation, the elastic-scattering and electron-transfer amplitude may be obtained from appropriate linear combinations of the collision amplitudes resulting from the gerade and the ungerade potential interactions. The differential cross section then takes the expression, for elastic scattering,

$$\frac{d\sigma_s}{d\Omega} = \frac{d\sigma_g}{d\Omega} + \frac{d\sigma_u}{d\Omega} + \frac{d\sigma_I}{d\Omega} \qquad (8.2)$$

and, for electron transfer,

$$\frac{d\sigma_{et}}{d\Omega} = \frac{d\sigma_g}{d\Omega} + \frac{d\sigma_u}{d\Omega} - \frac{d\sigma_I}{d\Omega} \tag{8.3}$$

with

$$\frac{d\sigma_g}{d\Omega} = 4\pi^4 \, |Tg|^2 \tag{8.4}$$

$$\frac{d\sigma_u}{d\Omega} = 4\pi^4 M \, |Tu|^2 \tag{8.5}$$

$$\frac{d\sigma_I}{d\Omega} = 8\pi^4 M \, \mathrm{Re}\{Tg \, Tu\} \tag{8.6}$$

where $\frac{d\sigma_g}{d\Omega}$, $\frac{d\sigma_u}{d\Omega}$ and $\frac{d\sigma_I}{d\Omega}$ correspond to the contributions to the cross section coming from the gerade interaction, the ungerade interaction and their interference.

Calculations of the differential cross section are carried out in the classical limit of the eikonal approximation for the "straight-line" and classical [to the order $|\beta|^3 a_o$] trajectories as well as for the "angle" approximation (Sec. VII). More specifically we will adopt the classical scattering matrix [Eq. (5.20)] obtained from the eikonal expression given by Eq. (5.11) [to $\mathcal{O}(\eta_s)$] by means of the stationary-phase approximation [Eq. (5.17)]. In paper III of this series, we shall illustrate the application of the eikonal approximation to scatterings where the classical description fails.

The condition for the validity of the classical scattering is given by Eq. (1.25). In Fig. 8, the region of classical scattering obtained from Eq. (1.25) is displayed for both the gerade and the ungerade adiabatic potentials in the straight-line approximation. The classical region is then given by the areas lying below the curves labelled $\eta(\text{class.}) = 1$. It is seen that the gerade potential is more restrictive than the ungerade potential. This is clear since the gerade potential has an attractive portion and would give rise to rainbow scattering for which, as mentioned before, the classical description of scattering fails. From Fig. 8, it is apparent that collisions with impact parameters in the neighborhood of 2 to 3.4 a_o are essentially nonclassical. (It will be seen later that rainbow scattering corresponds to an impact parameter of about 2.7 a_o.) At very small impact parameters (i.e. at $b \to 0$), the $\eta(\text{class.}) = 1$ curves for both the gerade and the ungerade potentials dip down to effective zero energy. (Due to the scale in Fig. 8, it is indistinguishable from the E_{CM}-axis.)

Utilizing the known adiabatic potentials[18] the classical scattering angle may be determined as a function of the impact parameter. For straight-line trajectory where the impact parameter equals the distance of closest approach, this is particularly simple since the energy dependence of θ_c can be factored out [see Eq. (1.5)]. This permits us to define a reduced classical scattering angle $\theta_c(b)\ \zeta^{-2}$ which is energy independent. We have

$$\Theta_c(b)\,\zeta^{-2} = -\frac{b}{M}\int_o^\infty \frac{d}{dR_o}\left(\frac{V(R_o)}{Ry}\right)\frac{dZ}{R_o} + \mathcal{O}(\theta_c^2) \tag{8.7}$$

with

$$\zeta = \frac{\hbar}{a_o p}\left(\frac{M}{m}\right) \tag{8.8}$$

where ζ is a dimensionless quantity. In Fig. 9, we have plotted the reduced scattering angle as a function of impact parameter. It is seen that in the gerade mode of interaction we have at $b \cong 2.7\, a_o$ a minimum. This would give rise to a rainbow.

For classical trajectory, the relation between the impact parameter and the distance of closest approach is no longer simple. To order $|\beta^3|\, a_o$, they are related by Eq. (2.13b). This relationship is shown in Fig. 10. As expected the deviation from d = b straight line becomes more pronounced with decreasing energy. The classical scattering angle for H^+ on H along classical trajectory may be obtained to the accuracy of $\Phi(b)$. We have from Eq. (3.5)

$$\Theta_c = \zeta\left(\frac{m}{M}\right)\frac{d\Phi(b)}{db}$$

$$= -\zeta^2\left(\frac{m}{M}\right)\int_o^\infty \frac{d\bar{R}}{db}\,\frac{d}{d\bar{R}}\left\{E[\beta^2 - \beta^2(Z)] + \frac{V(\bar{R})}{Ry}\right\}dZ + \mathcal{O}(\theta_c^3) \tag{8.9}$$

where $\bar{R}$ is given by Eq. (3.3). The calculated Θ_c is compared with that obtained in the straight-line trajectory approximation in Table I.

In the stationary-phase approximation, the contributing impact parameters to the classical scattering are defined by Eq. (5.17). They are shown in Fig. 11 as a function of the classical scattering angle Θ_c for several center-of-mass energies. The corresponding stationary phase $\gamma(b_c)$ [see Eq. (5.16)]

$$\gamma(b_c) = \Phi(b_c) - e_1 p b_c \theta \tag{8.10}$$

are shown in Fig. 12. Differences are found in the stationary phases as predicted by the "straight-line" trajectory approximations and by the classical trajectory approximations. These differences should become appreciable in the interference pattern.

Having determined the impact parameters and the stationary phase we are now in position to evaluate the differential cross section. The result for elastic scattering and resonant electron-transfer cross section using the classical scattering matrix given by Eq. (5.20) is shown in Figs. 13 to 15 as a function of scattering angles for several center-of-mass energies. The regular pattern of oscillation comes from the inteference [Eq. (8.6)] between the gerade- and ungerade- mode of interactions. It is seen that the interference depends sensitively upon their phases. In Fig. 16 the constituent components [given by Eqs. (8.4) to (8.6)] of the differential cross sections are shown for one of the energies. As expected the interferenace term $d\sigma_I/d\Omega$ oscillates with increasing amplitude and rapidity as the scattering angle decreases. The sum of the elastic-

scattering and resonant electron-transfer differential cross sections denoted by $d\sigma_t/d\Omega$ is, however, a smooth function of the scattering angle.

For comparison, the results obtained in the "angle" approximation [Eq. (7.4)] are also included in these figures. It is observed that the "angle" approximation yields values which are consistently close to the values obtained from the more elaborate calculation following the classical trajectory up to the order $|\beta|^3 a_o$. This seems to suggest that the simple generalization of the "straight-line" approximation offered by the "angle" approximation do constitute a significant improvement.

At angles smaller than the rainbow angle, the one-to-one relation between the impact parameter and scattering angle as shown in Fig. 11 for the stationary-phase approximation is no longer satisfied. The scattering observed at a single angle arises from the scatterings through several separated impact parameters. This would then give rise to interesting interference patterns. Such a behavior is expected for scatterings due to the gerade mode of interaction. In Fig. 17, the relation [Eq. (5.17)] between the impact parameters and the scattering angles is given for several center-of-mass energies. It is clear that at angles smaller than the rainbow angle Θ_r, there are three participating impact parameters for gerade scattering. For the ungerade scattering where the potential is repulsive and has no rainbow scattering, only one impact parameter participates for each scattering angle. Their corresponding stationary phases $\gamma(b_c)$ are given in Fig. 18.

To account for the scatterings coming from separated impact parameters in the gerade case, Eqs. (8.4) and (8.5) must be modified. We have

$$\frac{d\sigma_g}{d\Omega} = 4\pi^4 M \left| \sum_j T_{jg} \right|^2 \tag{8.11}$$

$$\frac{d\sigma_I}{d\Omega} = 8\pi^4 M \, \mathrm{Re}\left\{ \sum_j T_{jg} \, T_u \right\} \tag{8.12}$$

where the sum over j runs over all the particpating impact parameters for each scattering angle. Results for $d\sigma_g/d\Omega$ and $d\sigma_I/d\Omega$ calculated from these equations are given in Fig. 19. The interference structure in $d\sigma_g/d\Omega$ is apparent. This interference within the gerade scattering also gives rise to further structure in $d\sigma_I/d\Omega$. Superimposed on the regular gerade-ungerade oscillations in $d\sigma_I/d\Omega$ are the oscillations coming from interference within the gerade scattering. The elastic scattering and resonant electron-transfer differential cross sections at these scattering angles are shown in Fig. 20. The differences in the differential cross section at these small angles coming from the "straight-line" approximation, the "angle" approximation and the classical trajectory are small and become indistinguishable in these figures.

An investigation of the energy dependence of the differential cross sections has also been carried out. The results are given in Figs. 21 to 24 for a few scattering angles in the "straight-line" and the "angle"

approximations. In general the behavior of these quantities as a function of energy is similar to that as a function of scattering angles. For a fixed scattering angle, the rainbow scattering appears at certain critical energies and below which again we observe interference coming from separated impact parameters. The result obtained from the "angle" approximation agree reasonably well with that obtained by following the classical trajectory for all the energies that we have checked.

To our knowledge, no experimental measurement on the differential cross section for H^+ and H is available in the literature for a direct comparison with the theoretical result. Detailed measurements on the electron transfer probability in the (H^+, H) collision system has been carried out by Helbig and Everhart.[19] This then provides an indirect assess of the theoretical result for the differential cross section.

The electron transfer probability P_{et} can be calculated from the differential cross section by the relation

$$P_{et} = \left(\frac{d\sigma_{et}}{d\Omega}\right) \Big/ \left(\frac{d\sigma_{total}}{d\Omega}\right) \tag{8.13}$$

where $d\sigma_{total}/d\Omega$ is the total differential cross section for the (H^+, H) collision system. In the two-state approximation , the total differential cross section is approximated by $d\sigma_t/d\Omega$. Hence

$$\frac{d\sigma_{total}}{d\Omega} \cong \frac{d\sigma_t}{d\Omega} = \frac{d\sigma_{et}}{d\Omega} + \frac{d\sigma_s}{d\Omega} \tag{8.14}$$

In this approximation, the differential excitation cross sections are neglected.

The calculated electron transfer probability P_{et} is compared with the experimental measurements in Fig. 25 as a function of the incident proton energy for several fixed scattering angles and in Fig. 26 as a function of the scattering angle for several fixed incident proton energies. It is seen from Fig. 25 that the agreement between the theoretical and experimental electron-transfer probability as a function of proton energy is not quantitative. The improvement over the straight-line approximation introduced by the "angle" approximation in the positions of the oscillation is too small. No further appreciable improvement is obtained if the classical trjectory is followed up to the order $|\beta|^3 a_o$. The theoretical result also fails to predict the Everhart damping.[20] These are, however, expected of the adiabatic two-state approximation as was pointed out by a number of workers.[21-25] The discrepancy (displayed in Fig. 25) which is apparently larger than the experimental uncertainty comes partly from the approximation in $d\sigma_{total}/d\Omega$ as given by Eq. (8.14) and partly from the inaccuracy in the calculated differential cross sections as a result of the classical and adiabatic two-state approximations.

The agreement between the theoretical and experimental electron-transfer probability is, however, much better as a function of scattering angle, except for the case with an incident proton energy of 151 ev (the lowest energy measured). This agreement appears to be further improved

by the "angle" approximation. However experimental measurements of P_{et} at angles larger than those reported are needed to settle this point. At angles smaller than the rainbow angle, a increase in the oscillation in P_{et} is found. This increase is originated from the interference in the gerade scattering coming from separated impact parameters. A calculation of P_{et} following the classical trajectory up to the order $|\beta|^3 a_o$ is carried out as a function of scattering angle for two-fixed incident proton energies at 151 ev and 410 ev. The result is in good agreement with that obtained in the "angle" approximation. This further supports our observation mentioned earlier that the "angle" approximation, despite its simplicity, constitutes a significant improvement over the "straight-line" approximation.

REFERENCES

1. J. C. Y. Chen and K. M. Watson, Phys. Rev. 174, 152 (1968). This reference will be referred to as I and equations from I referenced as "Eq. (I1.1)", etc.
2. The extension of our methods to nonspherically symmetric potentials is straightforward.
3. See, for example, M. L. Goldberger and K. M. Watson, Collision Theory (John Wiley & Sons, Inc., New York, 1964) for a description of the functions $\psi_{\underset{\sim}{p}}^{\pm}$.
4. The condition (1.3) is usually quoted as that required for the validity of the eikonal approximation. The condition (1.14) is obtained in Appendix A, making use of our condition (1.2).
5. G. Moliere, Z. für Naturforschung 2A, 133 (1947).
6. S. Fernbach, R. Serber, and T. Taylor, Phys. Rev. 75, 1352 (1949).
7. K. M. Watson, Phys. Rev. 89, 575 (1953); N. C. Francis and K. M. Watson, Phys. Rev. 92, 291 (1953) and Am. J. Phys. 21, 659 (1953).
8. R. Glauber, "Lectures in Theoretical Physics," Vol. 1 (Interscience Publishers, Inc., N. Y., 1959).
9. D. R. Bates and A. R. Holt, Proc. Roy. Soc. (London) A292, 168 (1966).
10. F. T. Smith, J. Chem. Phys. 42, 2419 (1965); F. T. Smith, R. P. Marchi, and K. G. Dedrick, Phys. Rev. 150, 79 (1966).

11. L. Wilets and S. J. Wallace, Phys. Rev. 169, 84 (1968).

12. H. Goldstein, Classical Mechanics (Addison-Wesley Publishing Co., Inc., 1950), Chapter 7.

13. K. W. Ford and J. A. Wheeler, Ann. Phys. (N.Y.) 7, 259 (1959).

14. Equation (7.4) gives us Φ in the "angle" approximation. Dropping the term $2p\beta DU(d)$ gives us the "straight line" approximation.

15. D. R. Bates, K. Ledsham and A. L. Stewart, Phil. Trans. Roy. Soc. (London) 246, 215 (1953); see also J. M. Peek, J. Chem. Phys. 43, 3004 (1965).

16. H. S. W. Massey and R. A. Smith, Proc. Roy. Soc. (London) A142, 142 (1933).

17. W. Aberth, D. C. Lorents, R. P. Marchi and F. T. Smith, Phys. Rev. Letters 14, 776 (1965).

18. In the calculation accurate analytic fits to the exact adiabatic $^2\Sigma_g^+$ and $^2\Sigma_u^+$ H_2^+ potential curves (Ref. 15) are used. The united-atom limits for these H_2^+ states are properly incorporated in the analytic fits. We are grateful to Dr. C. S. Wang for his help in the analytic fitting of the potential.

19. H. F. Helbig and E. Everhart, Phys. Rev. 140, A715 (1965); see also G. J. Lockwood and E. Everhart, Phys. Rev. 125, 567 (1962).

20. See for example, F. P. Ziemba, G. J. Lockwood, G. H. Morgan and E. Everhart, Phys. Rev. 118, 1552 (1960); G. J. Lockwood and E. Everhart, Phys. Rev. 125, 567 (1962).

21. D. R. Bates and D. A. Williams, Proc. Phys. Soc. (London) 83, 425 (1964).

22. F. J. Smith, Proc. Phys. Soc. (London) 84, 889 (1964).

23. R. P. Marchi and F. T. Smith, Phys. Rev. 139, A1025 (1965).

24. W. Lichten, Phys. Rev. 131, 229 (1963); 139, A27 (1965).

APPENDIX A

The Error Resulting from the Eikonal Approximation

The error resulting from the use of the eikonal approximation may be estimated by replacing A in Eqs. (1.8a) and (1.12) by the product $A'A$. Here A is given by Eq. (1.8c) and A' represents a correction to this. The exact equation to determine A' is [see Eq. (I 4.31)]

$$\frac{\partial \ell n\, A'}{\partial x_3} = -(2\, A'A\, \kappa i)^{-1} \nabla^2 (A'A) \,. \tag{A.1}$$

To estimate A', we set $A' = 1$ on the right-hand side of (A.1). Using Eq. (1.8c), we obtain

$$A_1 \approx \exp\left\{\frac{i}{4\kappa}\left[\left(\frac{1}{R_1} + \frac{1}{R_2}\right) + \frac{\partial\, \ell n\, \kappa}{\partial x_3}\right]\right\}, \tag{A.2}$$

from which the estimate (1.14) follows.

Table I. Comparison of the scattering angle as a function of the impact parameter in the "straight-line" and the "classical trajectory $O(|\beta|^3 a_o)$" approximations.

$B_g(a_o)$	Θ_g	θ_g	$B_u(a_o)$	Θ_u	θ_u
E_{CM} = 75.5 ev			E_{CM} = 75.5 ev		
.53714	3.4633×10^{-1}	4.4610×10^{-1}	.40643	5.7277×10^{-1}	9.1860×10^{-1}
.76686	1.9749×10^{-1}	2.2679×10^{-1}	.61844	4.7074×10^{-1}	6.2399×10^{-1}
.98764	1.1065×10^{-1}	1.1871×10^{-1}	.82942	3.9215×10^{-1}	4.7957×10^{-1}
1.20264	5.6279×10^{-2}	5.7015×10^{-2}	1.04047	3.3247×10^{-1}	3.9066×10^{-1}
1.41358	2.0682×10^{-2}	1.8975×10^{-2}	1.25182	2.8537×10^{-1}	3.2791×10^{-1}
1.62147	-3.1303×10^{-3}	-5.3668×10^{-3}	1.46339	2.4677×10^{-1}	2.7957×10^{-1}
1.82702	-1.9067×10^{-2}	-2.1068×10^{-2}	1.67499	2.1427×10^{-1}	2.4023×10^{-1}
2.03073	-2.9509×10^{-2}	-3.1007×10^{-2}	1.88641	1.8637×10^{-1}	2.0715×10^{-1}
2.23299	-3.6017×10^{-2}	-3.6974×10^{-2}	2.09745	1.6216×10^{-1}	1.7881×10^{-1}
2.43411	-3.9677×10^{-2}	-4.0154×10^{-2}	2.30795	1.4100×10^{-1}	1.5429×10^{-1}
2.63435	-4.1273×10^{-2}	-4.1369×10^{-2}	2.51782	1.2244×10^{-1}	1.3299×10^{-1}
2.83392	-4.1387×10^{-2}	-4.1203×10^{-2}	2.72696	1.0616×10^{-1}	1.1448×10^{-1}
3.03298	-4.0455×10^{-2}	-4.0084×10^{-2}	2.93536	9.1885×10^{-2}	9.8390×10^{-2}
3.23166	-3.8808×10^{-2}	-3.8326×10^{-2}	3.14300	7.9381×10^{-2}	8.4435×10^{-2}
3.43009	-3.6694×10^{-2}	-3.6159×10^{-2}	3.34990	6.8455×10^{-2}	7.2354×10^{-2}
3.62835	-3.4301×10^{-2}	-3.3756×10^{-2}	3.55608	5.8929×10^{-2}	6.1919×10^{-2}
3.82652	-3.1767×10^{-2}	-3.1241×10^{-2}	3.76161	5.0645×10^{-2}	5.2912×10^{-2}
4.02464	-2.9194×10^{-2}	-2.8711×10^{-2}	3.96651	4.3459×10^{-2}	4.5188×10^{-2}
5.01587	-1.7653×10^{-2}	-1.7408×10^{-2}	4.98351	1.9855×10^{-2}	2.0264×10^{-2}
6.00939	-9.8121×10^{-3}	-9.7209×10^{-3}	5.99212	8.9006×10^{-3}	8.9907×10^{-3}
8.00290	-2.6907×10^{-3}	-2.6820×10^{-3}	7.99834	1.7437×10^{-3}	1.7476×10^{-3}

Table I. (Continued)

E_{CM} = 205 ev			E_{CM} = 205 ev		
.57921	1.3276×10^{-1}	1.4446×10^{-1}	.53580	2.3411×10^{-1}	2.6183×10^{-1}
.78878	7.4658×10^{-2}	7.8433×10^{-2}	.73880	1.8154×10^{-1}	1.9588×10^{-1}
.99583	4.1530×10^{-2}	4.2632×10^{-2}	.94193	1.4847×10^{-1}	1.5754×10^{-1}
1.20109	2.1008×10^{-2}	2.1126×10^{-2}	1.14530	1.2508×10^{-1}	1.3156×10^{-1}
1.40502	7.6706×10^{-3}	7.4452×10^{-3}	1.34891	1.0713×10^{-1}	1.1209×10^{-1}
1.60791	-1.1946×10^{-3}	-1.5007×10^{-3}	1.55267	9.2584×10^{-2}	9.6520×10^{-2}
1.80997	-7.0916×10^{-3}	-7.3696×10^{-3}	1.75649	8.0365×10^{-2}	8.3546×10^{-2}
2.01137	-1.0932×10^{-2}	-1.1142×10^{-2}	1.96029	6.9879×10^{-2}	7.2462×10^{-2}
2.21223	-1.3309×10^{-2}	-1.3445×10^{-2}	2.16400	6.0768×10^{-2}	6.2861×10^{-2}
2.41267	-1.4634×10^{-2}	-1.4703×10^{-2}	2.36756	5.2800×10^{-2}	5.4486×10^{-2}
2.61278	-1.5200×10^{-2}	-1.5215×10^{-2}	2.57092	4.5812×10^{-2}	4.7160×10^{-2}
2.81263	-1.5224×10^{-2}	-1.5200×10^{-2}	2.77406	3.9680×10^{-2}	4.0808×10^{-2}
3.01229	-1.4868×10^{-2}	-1.4818×10^{-2}	2.97696	3.4306×10^{-2}	3.5148×10^{-2}
3.21180	-1.4254×10^{-2}	-1.4188×10^{-2}	3.17962	2.9605×10^{-2}	3.0263×10^{-2}
3.41121	-1.3471×10^{-2}	-1.3398×10^{-2}	3.38203	2.5502×10^{-2}	2.6012×10^{-2}
3.61056	-1.2589×10^{-2}	-1.2514×10^{-2}	3.58420	2.1929×10^{-2}	2.2322×10^{-2}
3.80988	-1.1657×10^{-2}	-1.1584×10^{-2}	3.78615	1.8827×10^{-2}	1.9128×10^{-2}
4.00917	-1.0712×10^{-2}	-1.0645×10^{-2}	3.98789	1.6140×10^{-2}	1.6369×10^{-2}
5.00589	-6.4803×10^{-3}	-6.4468×10^{-3}	4.99399	7.3460×10^{-2}	7.4007×10^{-3}
6.00348	-3.6056×10^{-3}	-3.5932×10^{-3}	5.99711	3.2857×10^{-3}	3.2978×10^{-3}
8.00107	-9.9015×10^{-4}	-9.8898×10^{-4}	7.99939	6.4253×10^{-4}	6.4306×10^{-4}

FIGURE CAPTIONS

Fig. 1. Illustration of the eikonal trajectories and boundary conditions for ψ_p^+ and ψ_k^-.

Fig. 2. Description of the trajectory in the (x,z) coordinate system.

Fig. 3. Trajectories in the coordinate systems (2.15) and (2.15 ψ^-) are illustrated in (a) and (b), respectively.

Fig. 4. Illustration of trajectory and eikonal surface through point R_0.

Fig. 5. Illustration of the displacement D of Eq. (2.19) and of the two surfaces of Eq. (2.20).

Fig. 6. Trajectory for the "angle" approximation.

Fig. 7. Comparison of the phase Φ for the potential (7.7) of the "straight line," "angle," and "exact" methods.

Fig. 8. The region of classical scattering for H^+ on H as predicted by Eq. (5.19) and the condition (1.25) in the "straight-line" trajectory approximation for the adiabatic $^2\Sigma_g^+$(———) and $^2\Sigma_u^+$(----) H_2^+ potentials.

Fig. 9. The impact-parameter dependence of the reduced classical scattering angle $\Theta\,\zeta^{-2}$ as given by Eq. (8.7) for the adiabatic $^2\Sigma_g^+$ and $^2\Sigma_u^+$ H_2^+ potentials.

Fig. 10. The relation between the distance of closest approach and the impact parameters along the classical trajectory $[O(|\beta|^3\, a_o)]$ as given by Eq. (2.13b) for the "gerade" and the "ungerade" interactions for the (H^+,H) collision system at three center-of-mass energies.

Fig. 11. The stationary-phase impact parameter b_c as a function of the center-of-mass scattering angle for the (H^+,H) collision system at three center-of-mass energies. b_g and b_n denote those of the b_c's for the "gerade" and the "ungerade" modes of interactions, respectively. The differences in b_c found at these angles in the "straight-line," and the "classical trajectory" $[o(|\beta|^3 a_o)]$ approximation are too small to be seen for the scale adopted in the figure.

Fig. 12. Comparison of the stationary phase γ [Eq. (8.10)] as a function of the center-of-mass scattering angle in the "straight-line" (– – –), and "angle" (-----) and the "classical trajectory" $[o(|\beta|^3 a_o)]$ (———) approximations for the (H^+,H) collision system at three center-of-mass energies. The subscripts "g" and "u" denote the "gerade" and the "ungerade" potential of interaction, respectively.

Fig. 13. Comparison of the scattering and electron-transfer differential cross sections and their sum as functions of the scattering angles in the "straight-line" (– – –), the "angle" (-----) and the "classical trajectory" $[o(|\beta|^3 a_o)]$ (———) approximations for the (H^+,H) collision system at an energy of 75.5 eV in the center-of-mass system.

Fig. 14. Comparison of the scattering and electron-transfer differential cross sections and their sum as functions of the scattering angles in the "straight-line" (– – –), the "angle" (-----) and the "classical trajectory" $[o(|\beta|^3 a_o)]$ (———) approximations for the (H^+,H) collision system at an energy of 205 eV in the center-of-mass system.

Fig. 15. Comparison of the scattering and electron-transfer differential cross sections and their sum as functions of the scattering angles in the "straight-line" (– – –), the "angle" (-----) and the "classical trajectory" [$o(|\beta|^3 a_o)$] (———) approximations for the (H^+,H) collision system at an energy of 500 eV in the center-of-mass system.

Fig. 16. Comparison of the differential cross sections for the gerade-potential scattering, the ungerade-potential scattering and their interference [see Eqs. (8.4), (8.5) and (8.6), respectively] as functions of the scattering angle in the "straight-line" (– – –), the "angle" (-----) and the "classical trajectory" [$o(|\beta|^3 a_o)$] (———) approximations for the (H^+,H) collision system at an energy of 205 eV in the center-of-mass system.

Fig. 17. Comparison of the stationary-phase impact parameters b_c as a function of the absolute center-of-mass scattering angle $|\Theta_{CM}|$ in the "straight-line" (– – –) and the "classical trajectory" [$o(|\beta|^3 a_o)$] (———) approximations for the (H^+,H) collision system at two center-of-mass energies. b_g and b_n denote those of the b_c's for the "gerade" and the "ungerade" modes of interactions, respectively.

Fig. 18. The stationary phase γ [Eq. (8.10)] as a function of the absolute center-of-mass scattering angle $|\Theta_{CM}|$ for the (H^+,H) collision system at two center-of-mass energies. The subscripts "g" and "u" denote the "gerade" and the "ungerade" potential of interaction, respectively. The difference in γ found in the "straight-line," the "angle" and the "classical trajectory" [$o(|\beta|^3 a_o)$] approximation at these angles are too small to be seen for the scale adopted in the figure.

Fig. 19. The differential cross sections for the gerade-potential scattering, the ungerade-potential scattering and their interference [see Eqs. (8.11), (8.5) and (8.12), respectively] as functions of the scattering angle for the (H^+,H) collision system at an energy of 75.5 eV in the center-of-mass system. The difference in the differential cross section found in the "straight-line," the "angle" and the "classical trajectory" $[O(|\beta|^3 a_o)]$ approximations at these angles are too small to be seen for the scale adopted in the figure.

Fig. 20. The scattering and electron-transfer differential cross sections and their sum as functions of the scattering angle for the (H^+,H) collision system at an energy of 75.5 eV in the center-of-mass system. The difference in the differential cross sections found in the "straight-line," the "angle" and the "classical trajectory" $[O(|\beta|^3 a_o)]$ approximations at these angles are too small to be seen for the scale adopted in the figure.

Fig. 21. Comparison of the differential cross sections for the gerade-potential scattering, the ungerade-potential scattering and their interference [see Eqs. (8.4), (8.5) and (8.6), respectively] as functions of the energy for the (H^+,H) collision system in the "straight-line" (- - -) and the "angle" (———) approximations at a scattering angle of 6^o in the center-of-mass system.

Fig. 22. Comparison of the scattering and electron-transfer differential cross sections and their sum as functions of the energy in the "straight-line" (- - -) and the "angle" (———) approximations for the (H^+,H) collision system at a scattering angle of 4^o in the center-of-mass system.

Fig. 23. Comparison of the differential cross sections for the gerade-potential scattering, the ungerade-potential scattering and their interference [see Eqs. (8.11), (8.5) and (8.6), respectively] as functions of the energy in the "straight-line" (– – –) and the "angle" (———) approximations for the (H^+,H) collision system at a scattering angle of 2^o in the center-of-mass system.

Fig. 24. Comparison of the scattering and electron transfer differential cross sections and their sum for the (H^+,H) collision system as functions of the energy in the "straight-line" (– – –), and the "angle" (———) approximations at a scattering angle of 2^o in the center-of-mass system.

Fig. 25. Comparison of the calculated electron-transfer probability P_{et} in the (H^+,H) collision system as a function of the incident proton energy in the "straight-line" (– – –) and the "angle" (———) approximations with that measured by Helbig and Everhart[19] (crosses) at four laboratory scattering angles.

Fig. 26. Comparison of the calculated electron-transfer probability P_{et} in the (H^+,H) collision system as a function of the laboratory scattering angle in the "straight-line" (———) and the "angle" (-----) and the "classical trajectory" $[O(|\beta|^3 a_o)]$ (– – –) approximations with that measured by Helbig and Everhart[19] (crosses) at six incident proton energies. The "classical trajectory" $[O(|\beta|^3 a_o)]$ approximation is carried out only for the incident proton energy of 151 eV and 410 eV.

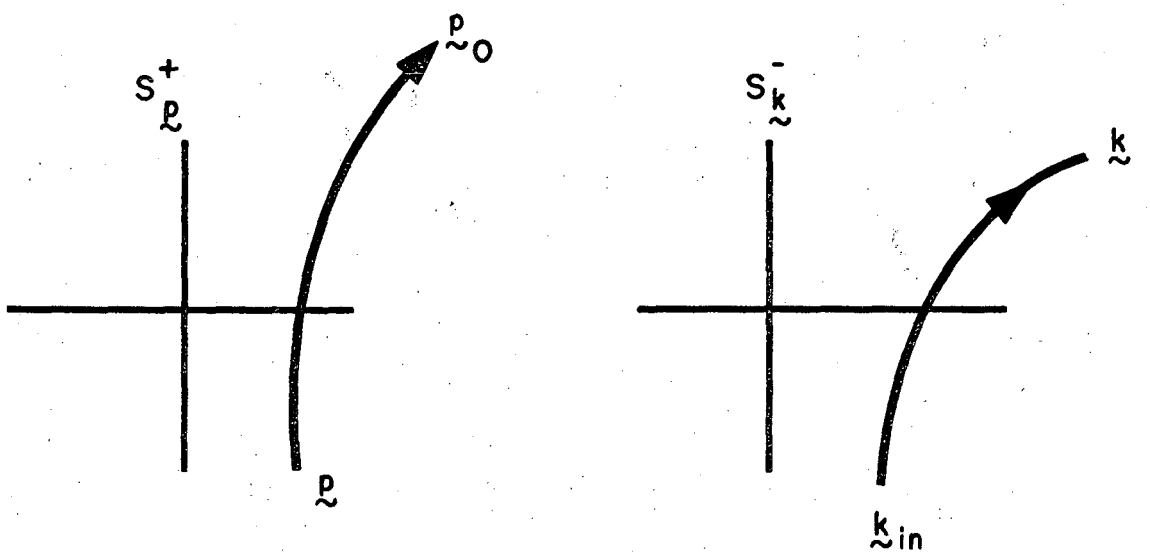
$S^+_{\underset{\sim}{p}}$
$\underset{\sim}{p}_o$
$\underset{\sim}{p}$
$S^-_{\underset{\sim}{k}}$
$\underset{\sim}{k}$
$\underset{\sim}{k}_{in}$
XBL6812-7332

Fig. 1

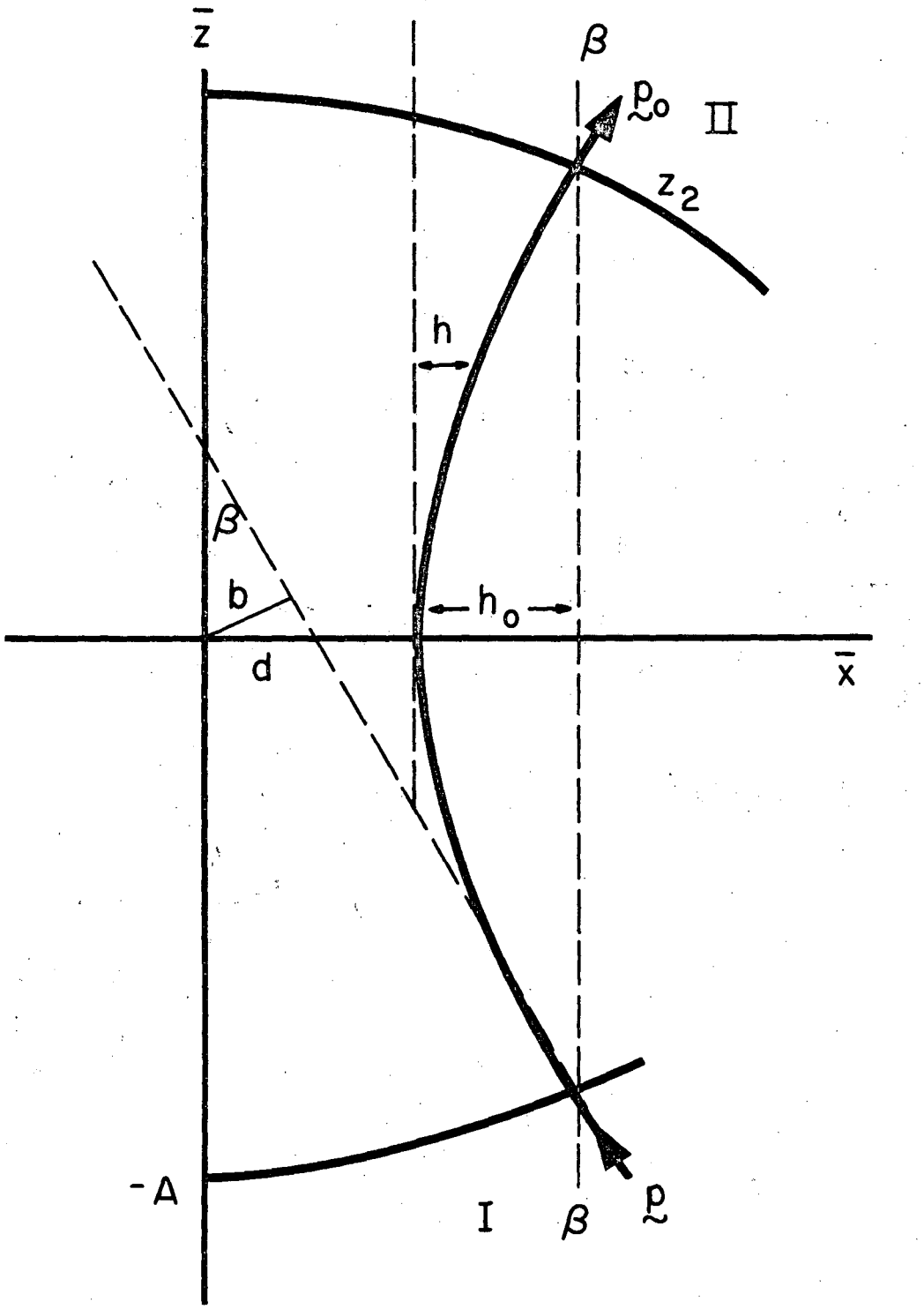

XBL6812-7334

Fig. 2a

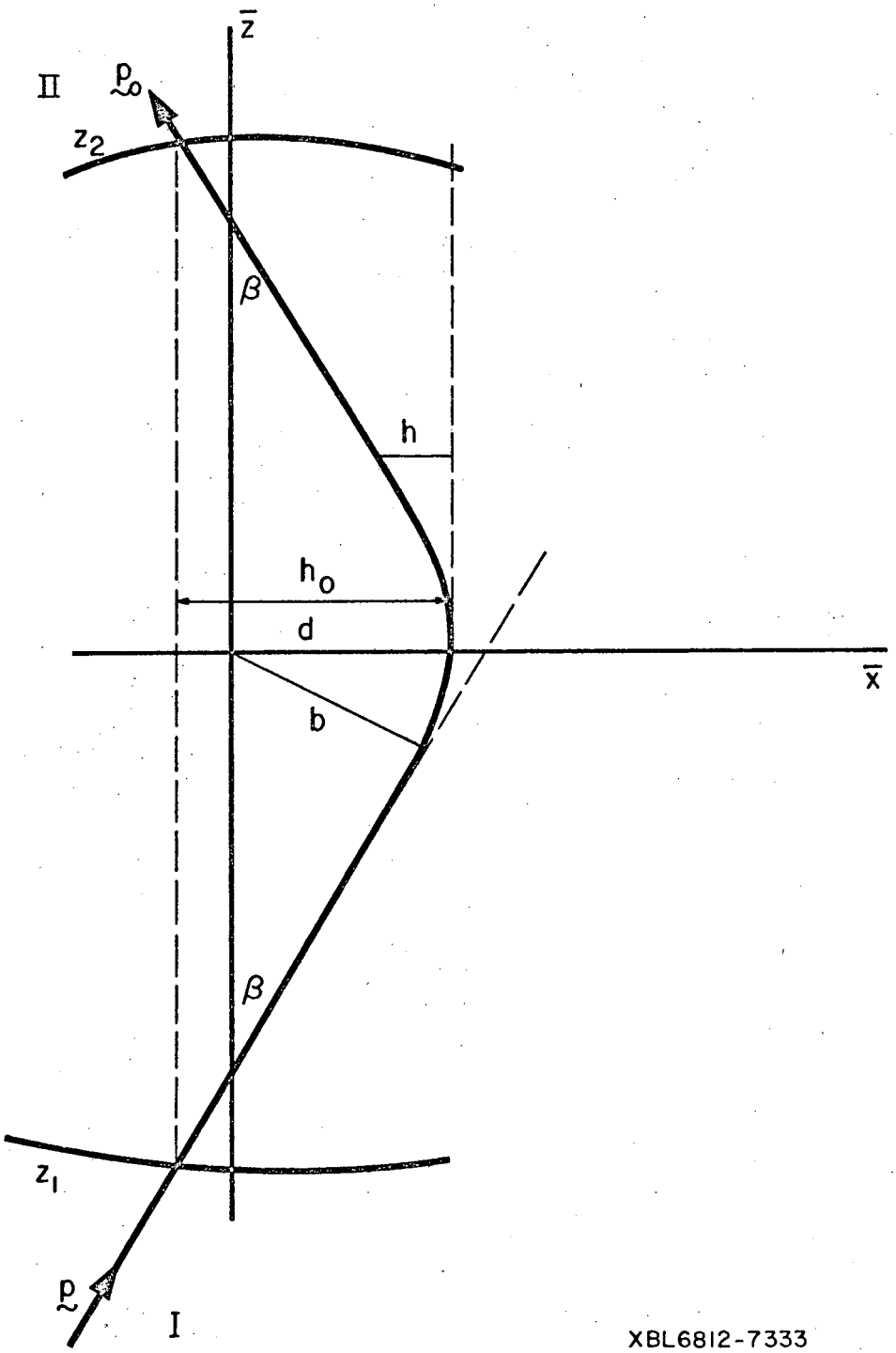

Fig. 2b

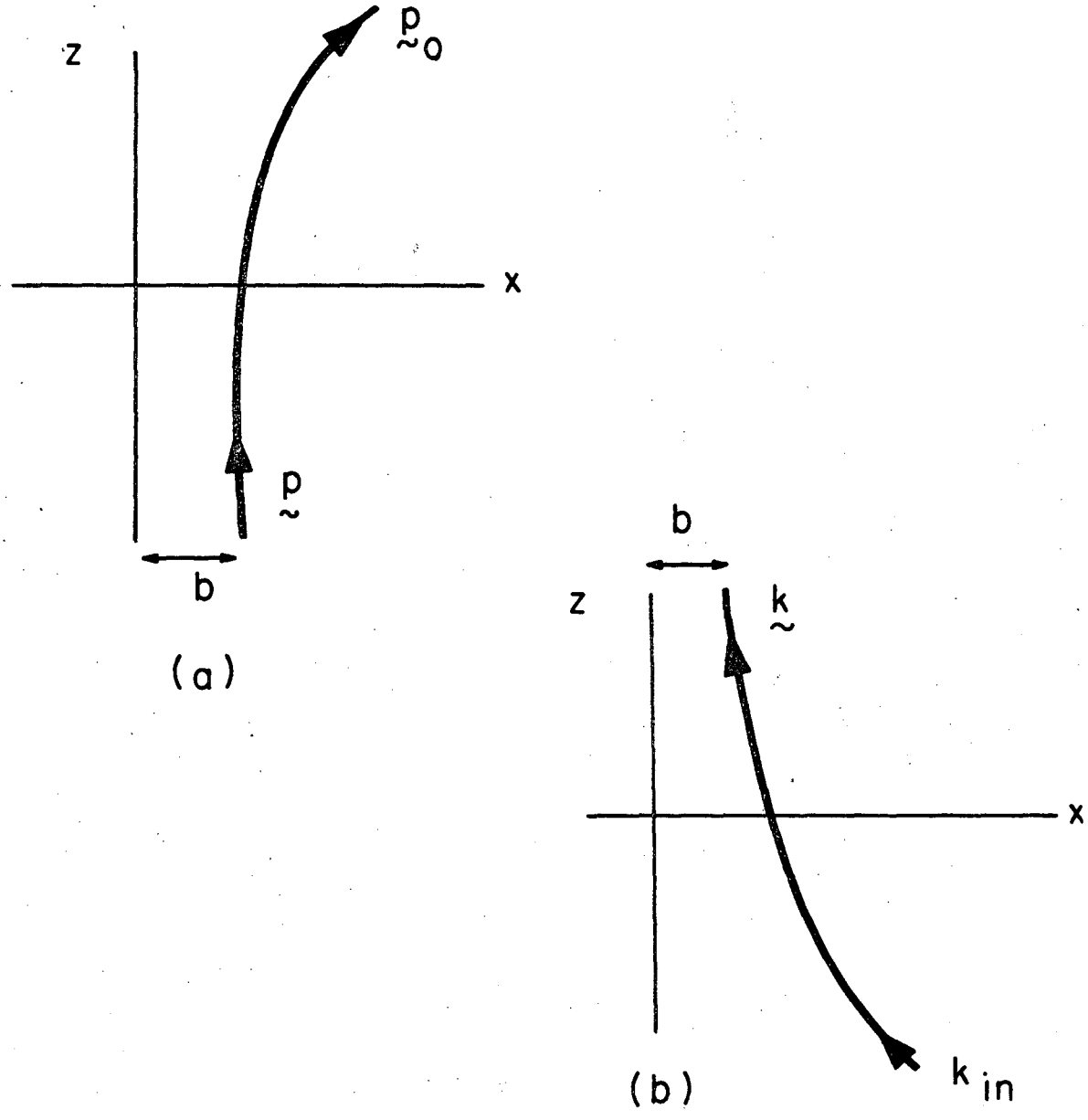

Fig. 3

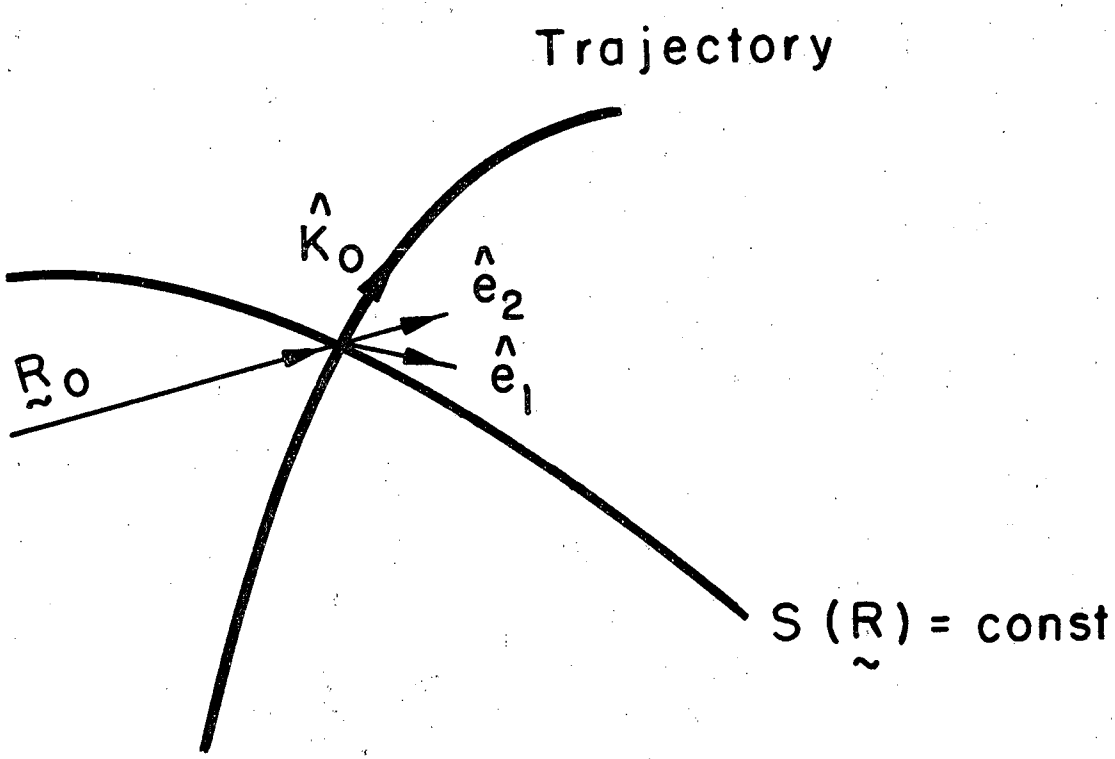

XBL691-1696

Fig. 4

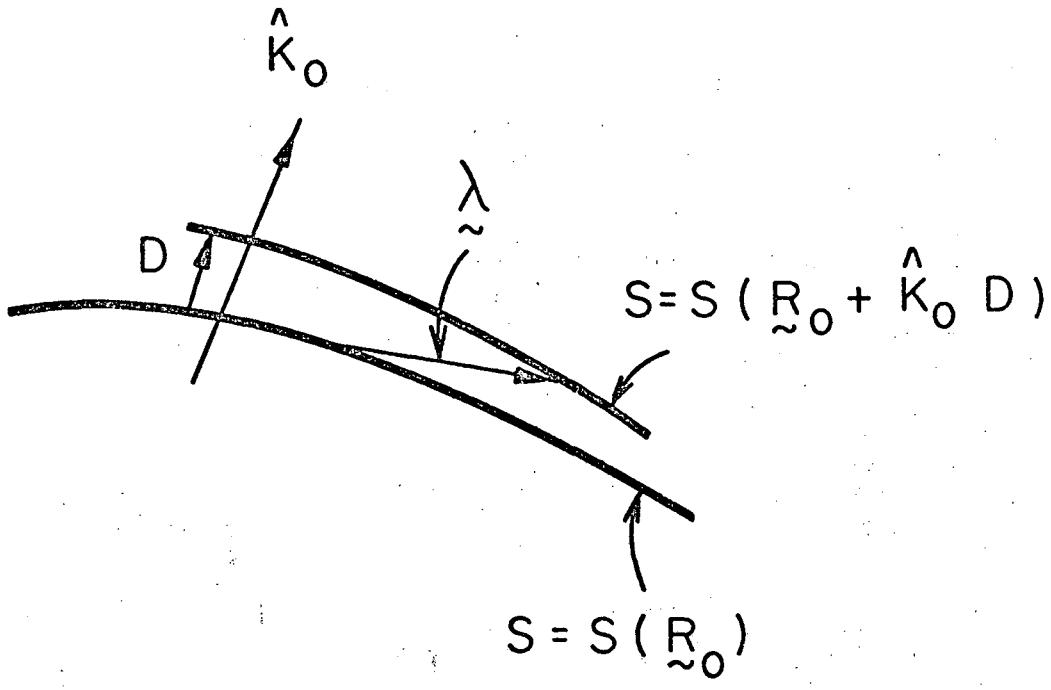

XBL691-1697

Fig. 5

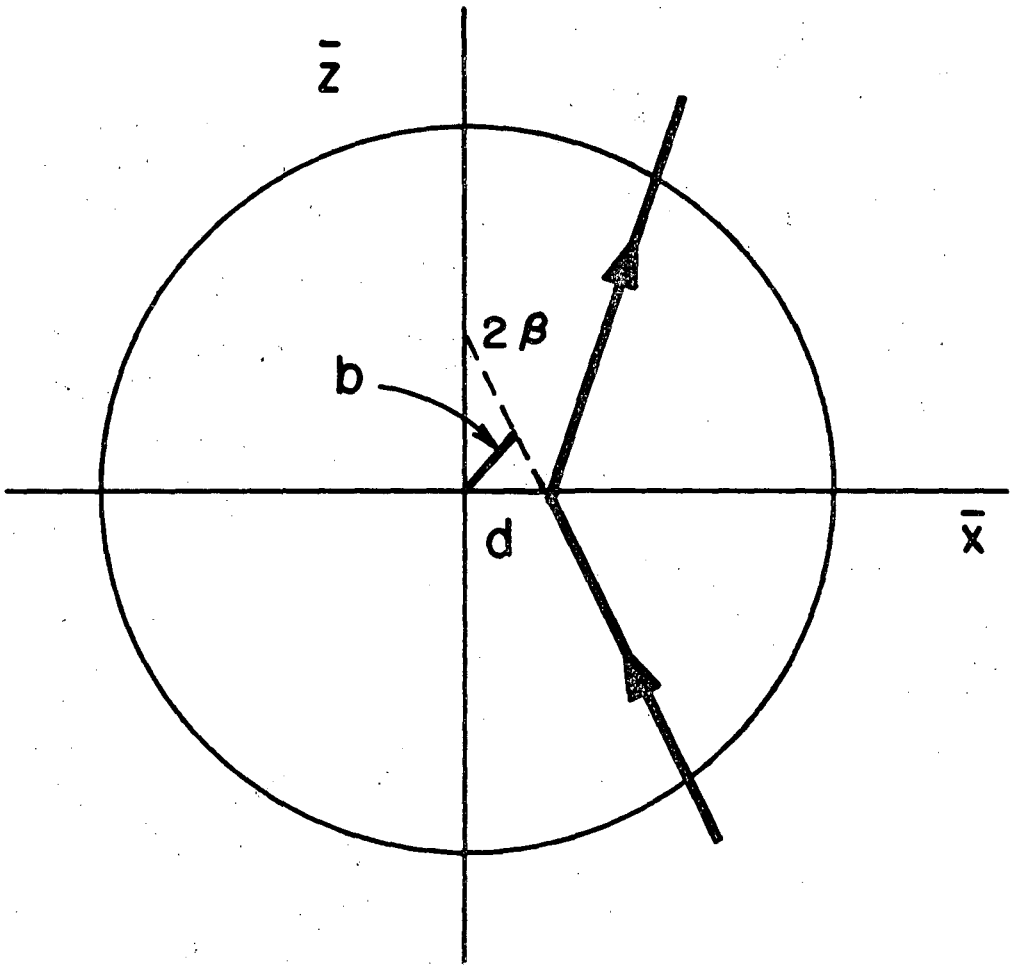

XBL691-1698

Fig. 6

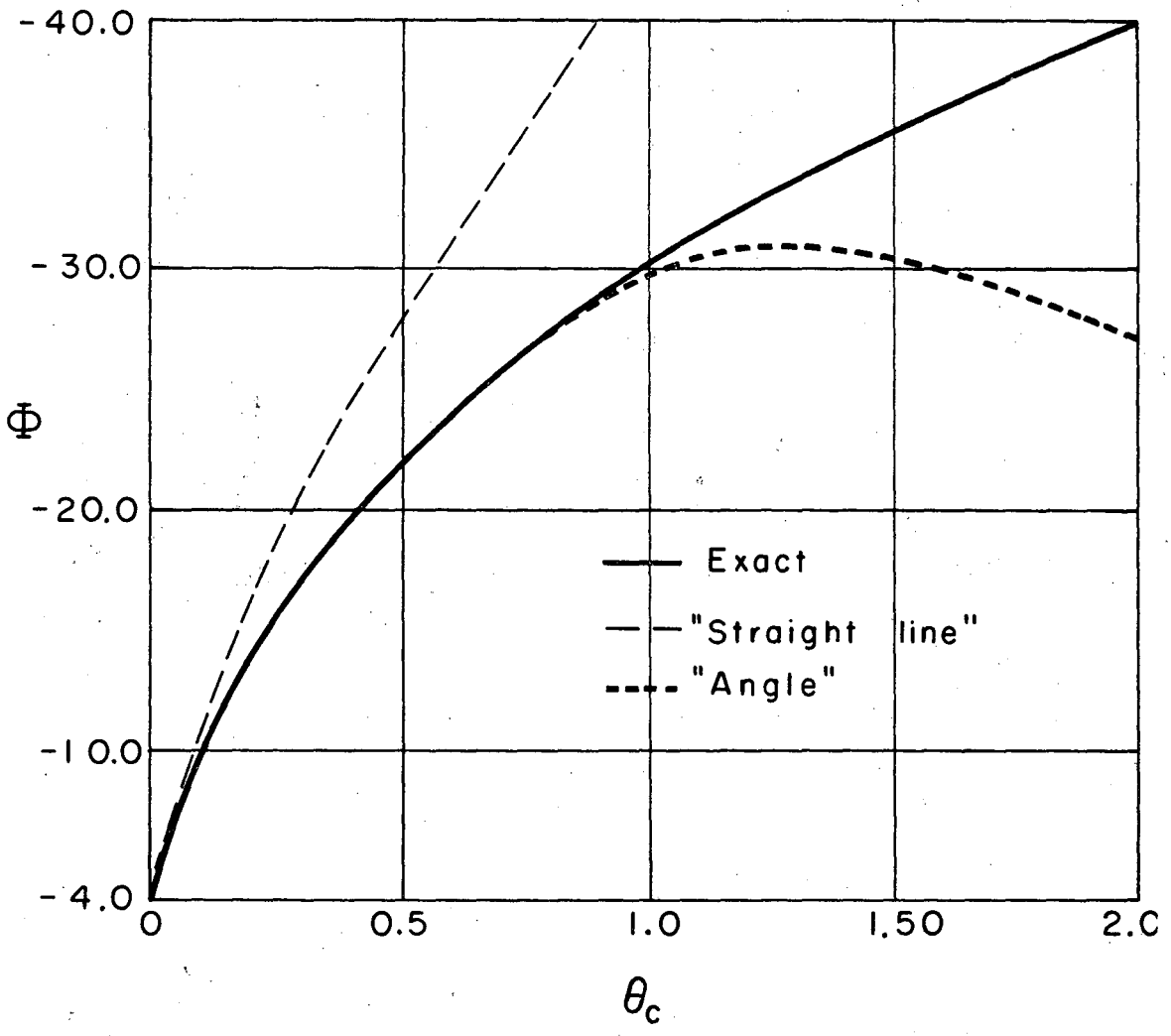
-40.0
-30.0
-20.0
-10.0
-4.0
Φ
0
0.5
1.0
1.50
2.0
θ_c
Exact
"Straight line"
"Angle"
XBL691-1699

Fig. 7

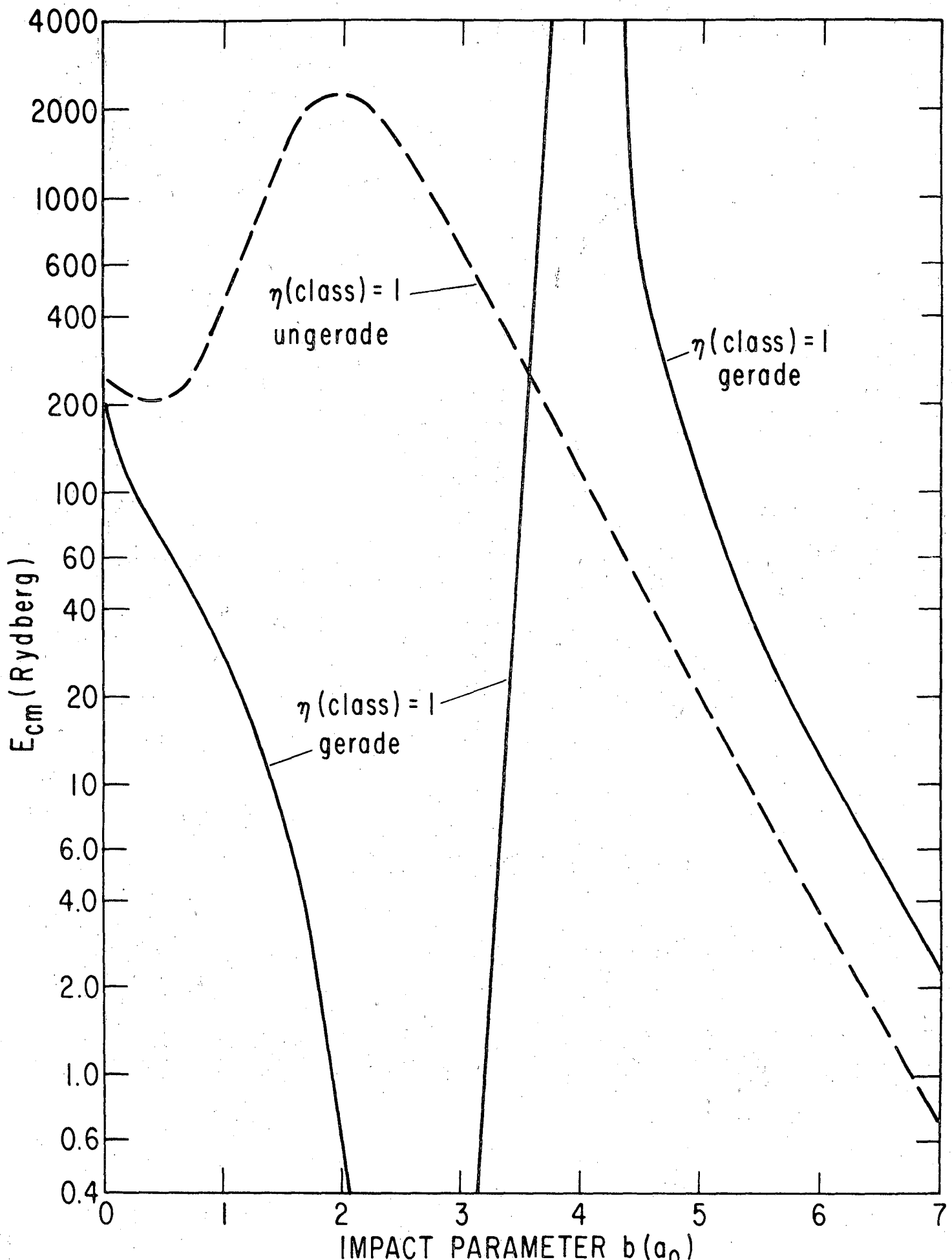
4000
2000
1000
600
400
200
100
60
40
20
10
6.0
4.0
2.0
1.0
0.6
0.4
E_{cm} (Rydberg)
η(class) = 1
ungerade
η(class) = 1
gerade
η(class) = 1
gerade
0
1
2
3
4
5
6
7
IMPACT PARAMETER b (a_0)

Fig. 8

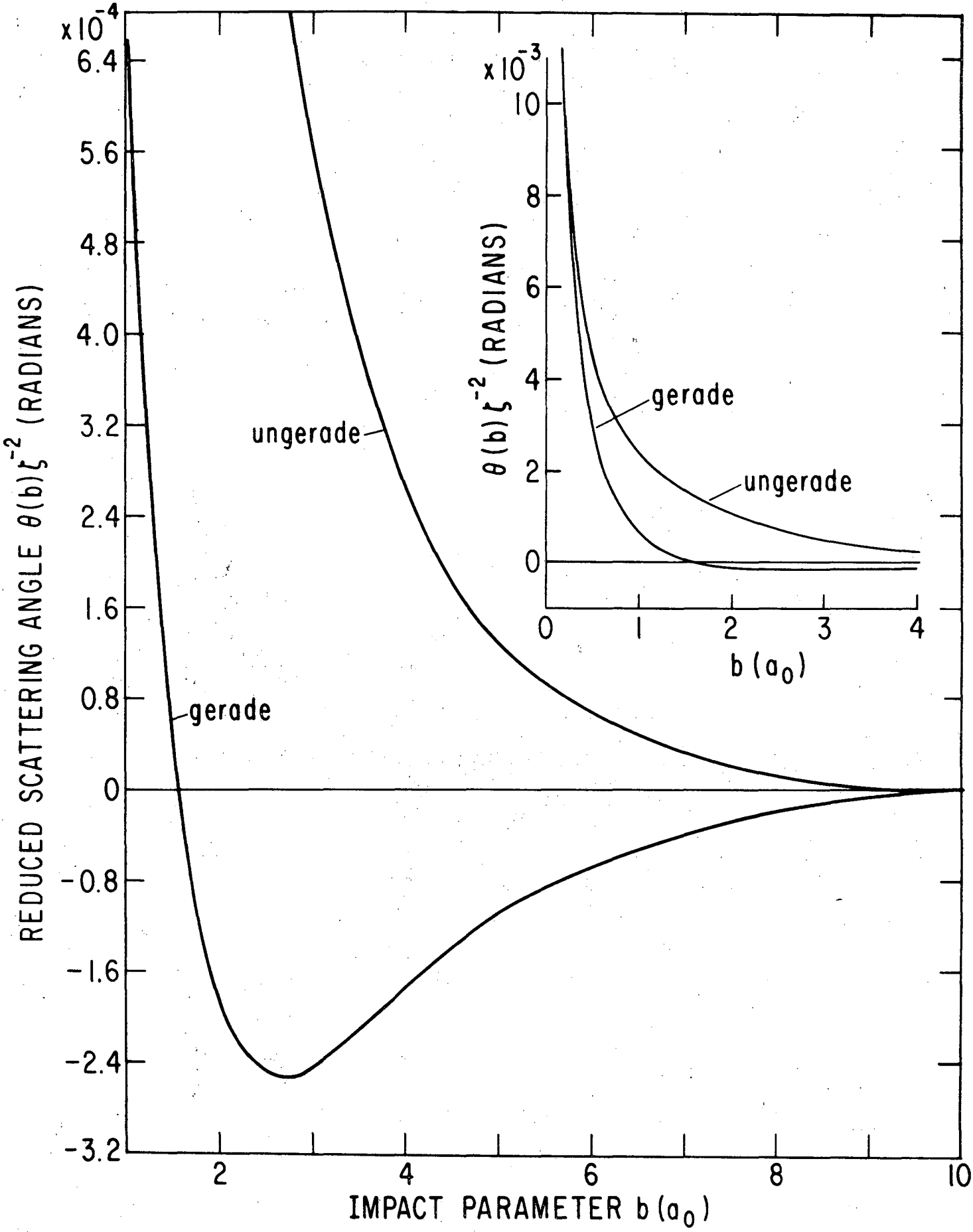
x10^-4
6.4
5.6
4.8
4.0
3.2
2.4
1.6
0.8
0
-0.8
-1.6
-2.4
-3.2
REDUCED SCATTERING ANGLE θ(b)ζ^-2 (RADIANS)
ungerade
gerade
2
4
6
8
10
IMPACT PARAMETER b(a0)
x10^-3
10
8
6
4
2
0
θ(b)ζ^-2 (RADIANS)
gerade
ungerade
0
1
2
3
4
b(a0)

Fig. 9

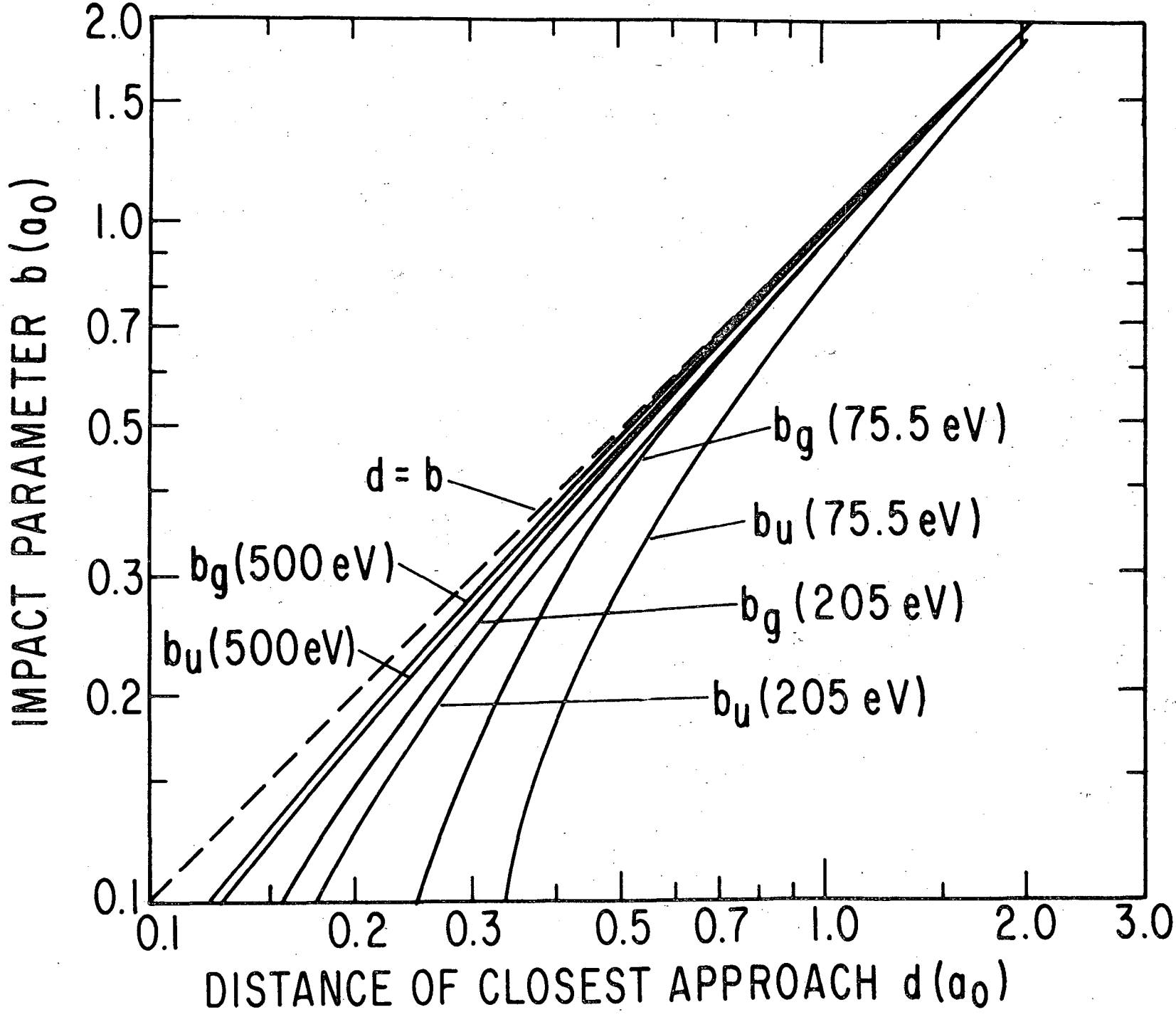
IMPACT PARAMETER b(a0)
DISTANCE OF CLOSEST APPROACH d(a0)
2.0
1.5
1.0
0.7
0.5
0.3
0.2
0.1
0.1
0.2
0.3
0.5
0.7
1.0
2.0
3.0
d = b
bg(500 eV)
bu(500eV)
bg (75.5 eV)
bu (75.5 eV)
bg (205 eV)
bu (205 eV)

Fig. 10

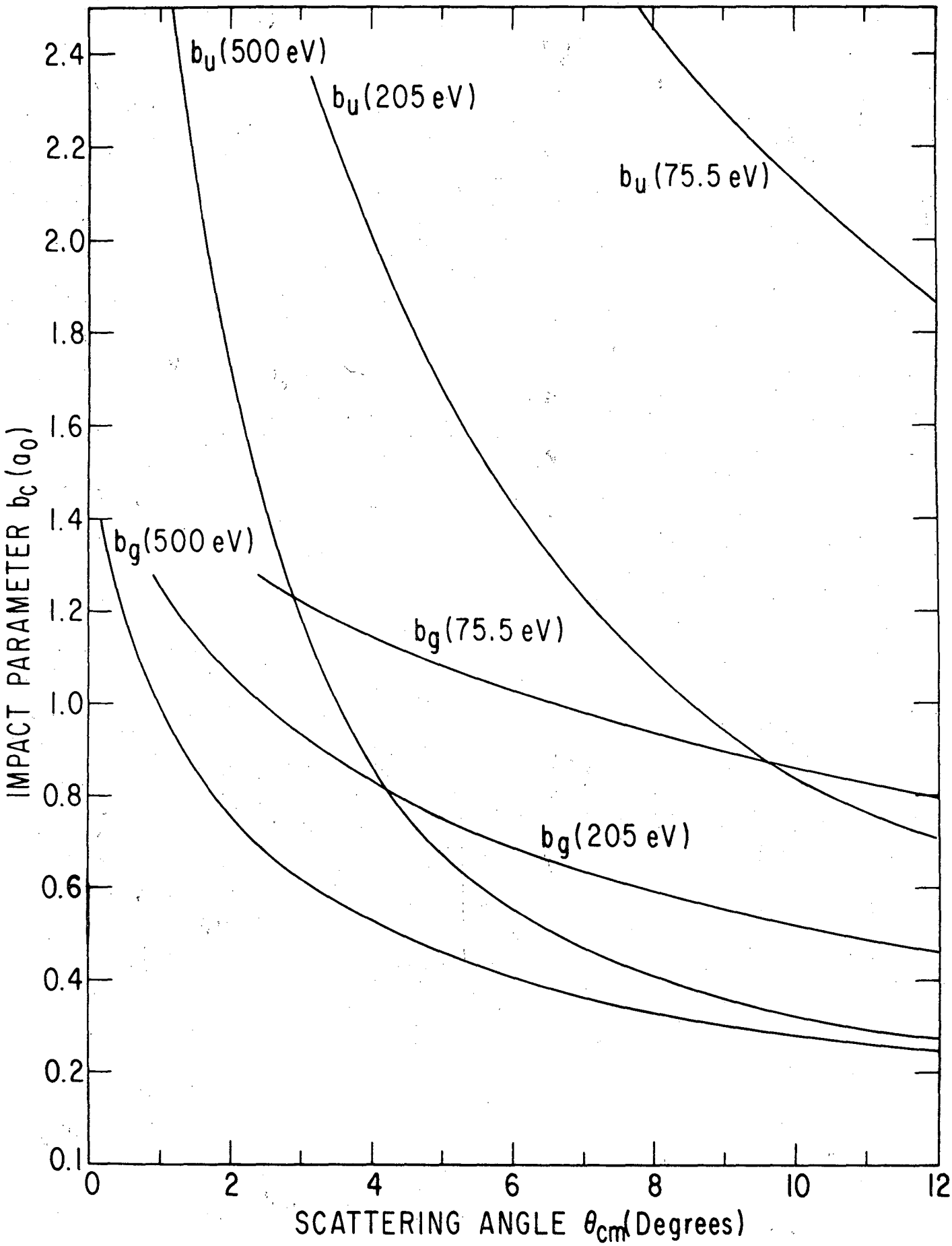
b_u(500 eV)
b_u(205 eV)
b_u(75.5 eV)
b_g(500 eV)
b_g(75.5 eV)
b_g(205 eV)
IMPACT PARAMETER b_c (a_0)
SCATTERING ANGLE θ_{cm}(Degrees)
2.4
2.2
2.0
1.8
1.6
1.4
1.2
1.0
0.8
0.6
0.4
0.2
0.1
0
2
4
6
8
10
12

Fig. 11

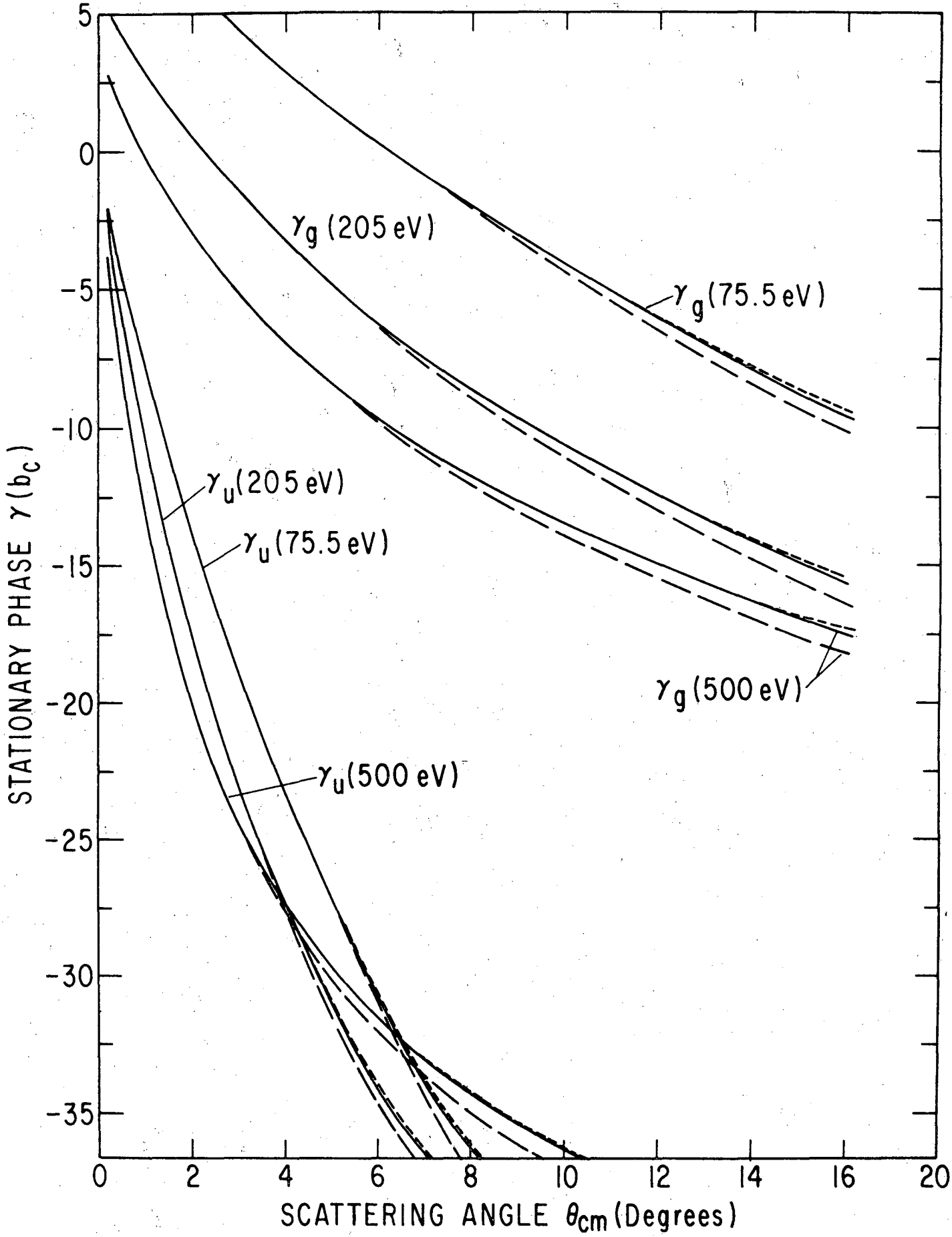
5
0
-5
-10
-15
-20
-25
-30
-35
STATIONARY PHASE γ(b_c)
γ_g (205 eV)
γ_g (75.5 eV)
γ_u (205 eV)
γ_u (75.5 eV)
γ_g (500 eV)
γ_u (500 eV)
0
2
4
6
8
10
12
14
16
20
SCATTERING ANGLE θ_cm (Degrees)

Fig. 12

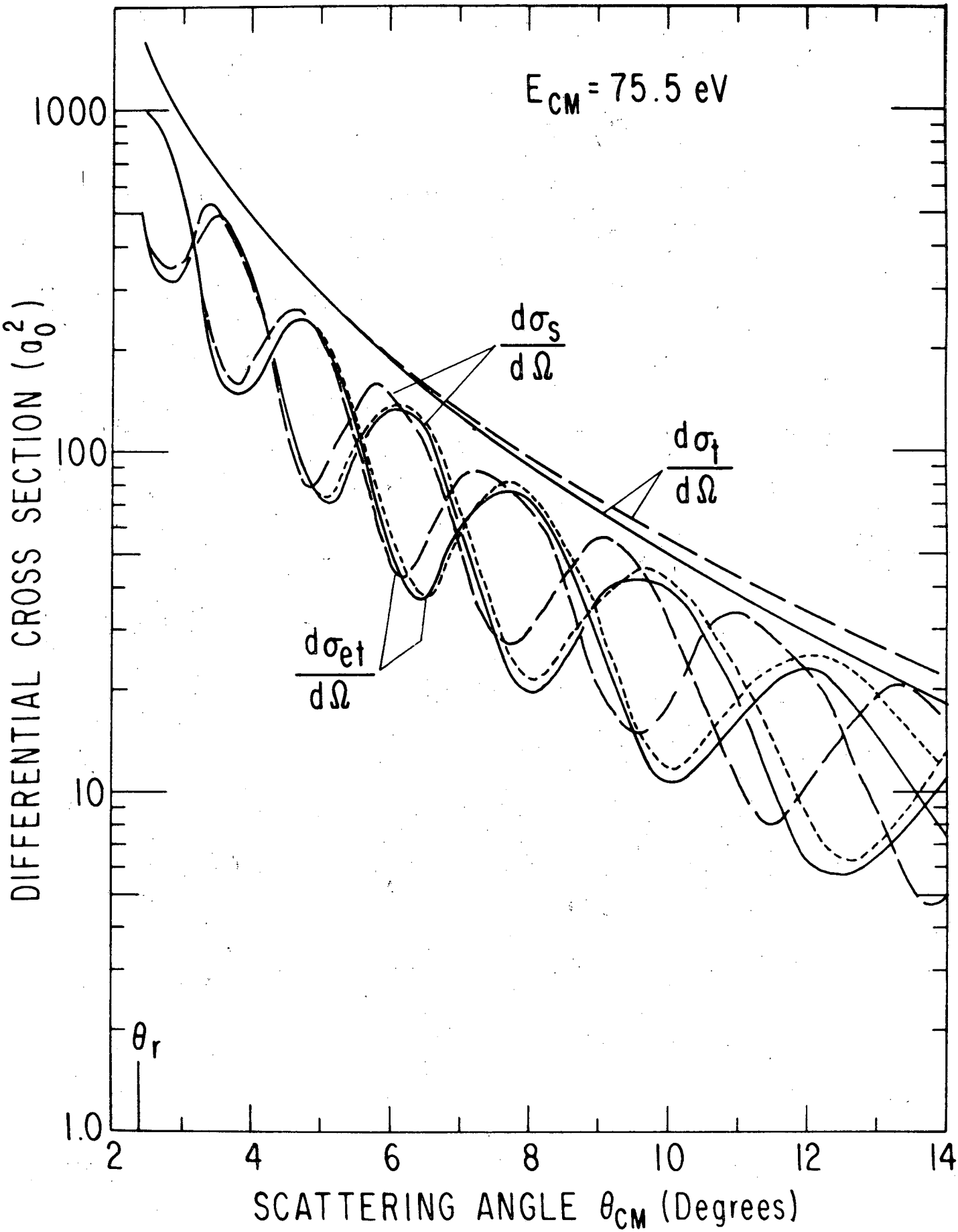
E_{CM} = 75.5 eV
$\frac{d\sigma_s}{d\Omega}$
$\frac{d\sigma_t}{d\Omega}$
$\frac{d\sigma_{et}}{d\Omega}$
θ_r
DIFFERENTIAL CROSS SECTION (a_0^2)
1000
100
10
1.0
2
4
6
8
10
12
14
SCATTERING ANGLE θ_{CM} (Degrees)

Fig. 13

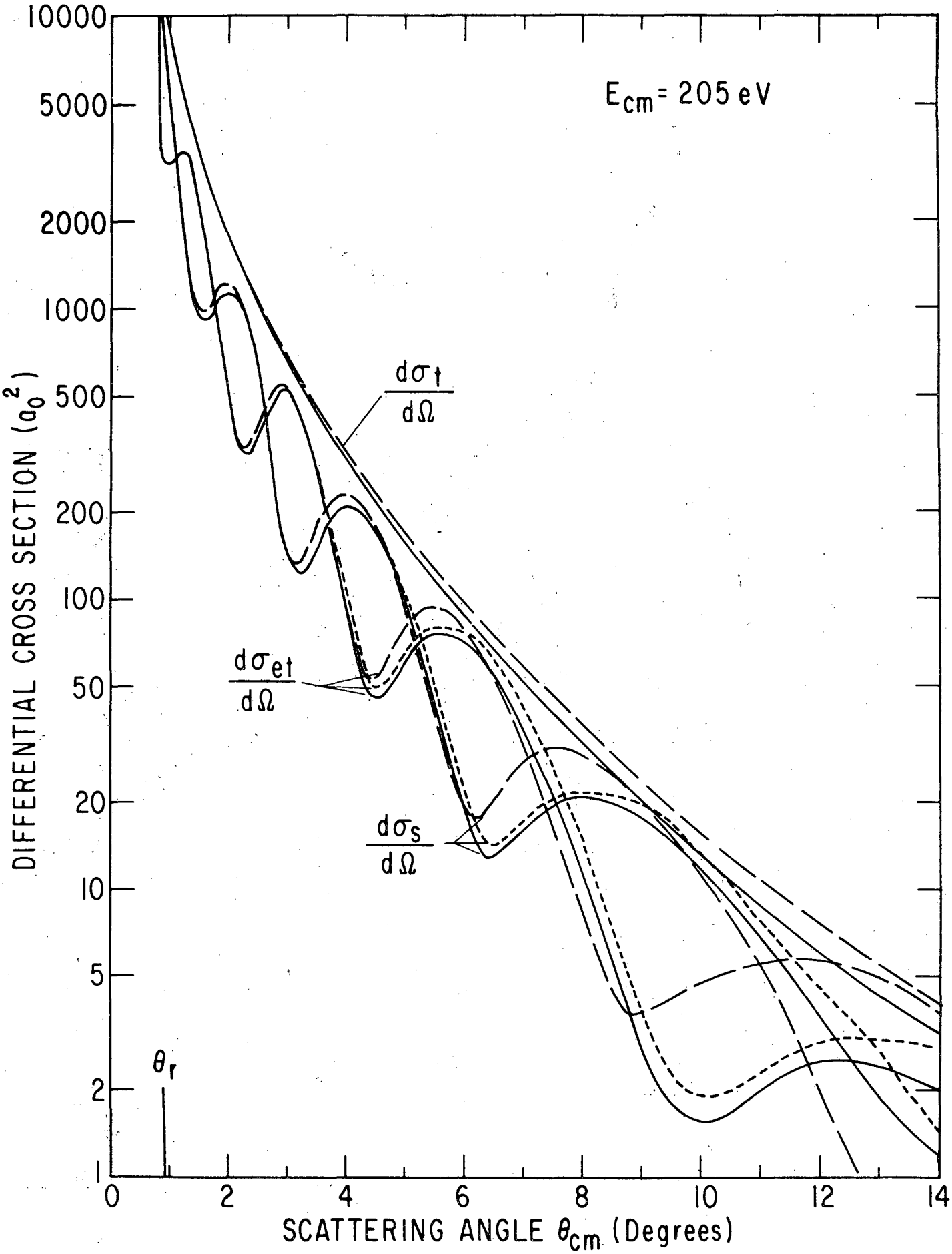
E_{cm} = 205 eV
$\frac{d\sigma_t}{d\Omega}$
$\frac{d\sigma_{et}}{d\Omega}$
$\frac{d\sigma_s}{d\Omega}$
θ_r
DIFFERENTIAL CROSS SECTION (a_0^2)
SCATTERING ANGLE θ_{cm} (Degrees)
10000
5000
2000
1000
500
200
100
50
20
10
5
2
1
0
2
4
6
8
10
12
14

Fig. 14

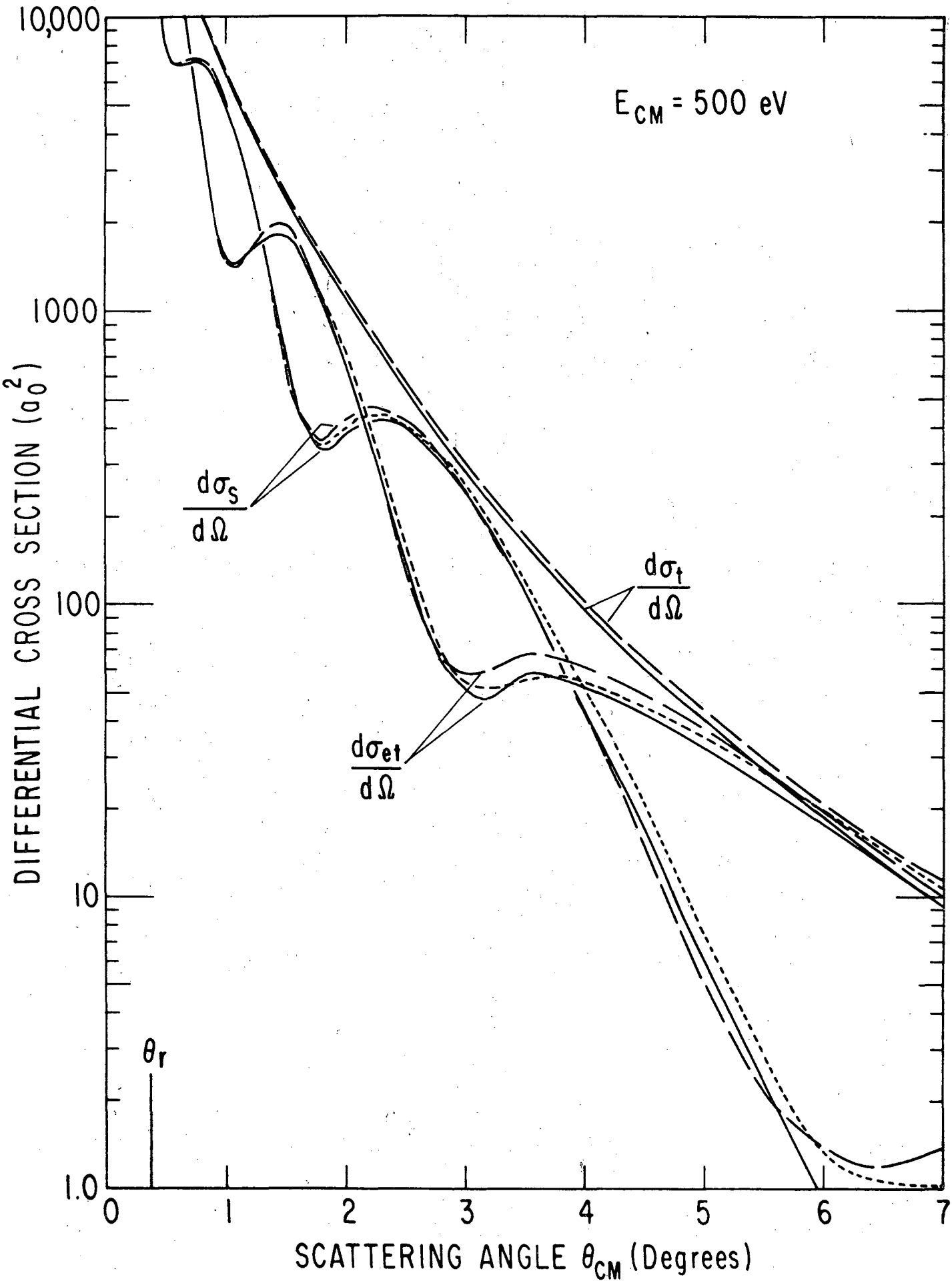
10,000
1000
100
10
1.0
DIFFERENTIAL CROSS SECTION (a_0^2)
E_{CM} = 500 eV
$\frac{d\sigma_s}{d\Omega}$
$\frac{d\sigma_t}{d\Omega}$
$\frac{d\sigma_{et}}{d\Omega}$
θ_r
0
1
2
3
4
5
6
7
SCATTERING ANGLE θ_{CM} (Degrees)

Fig. 15

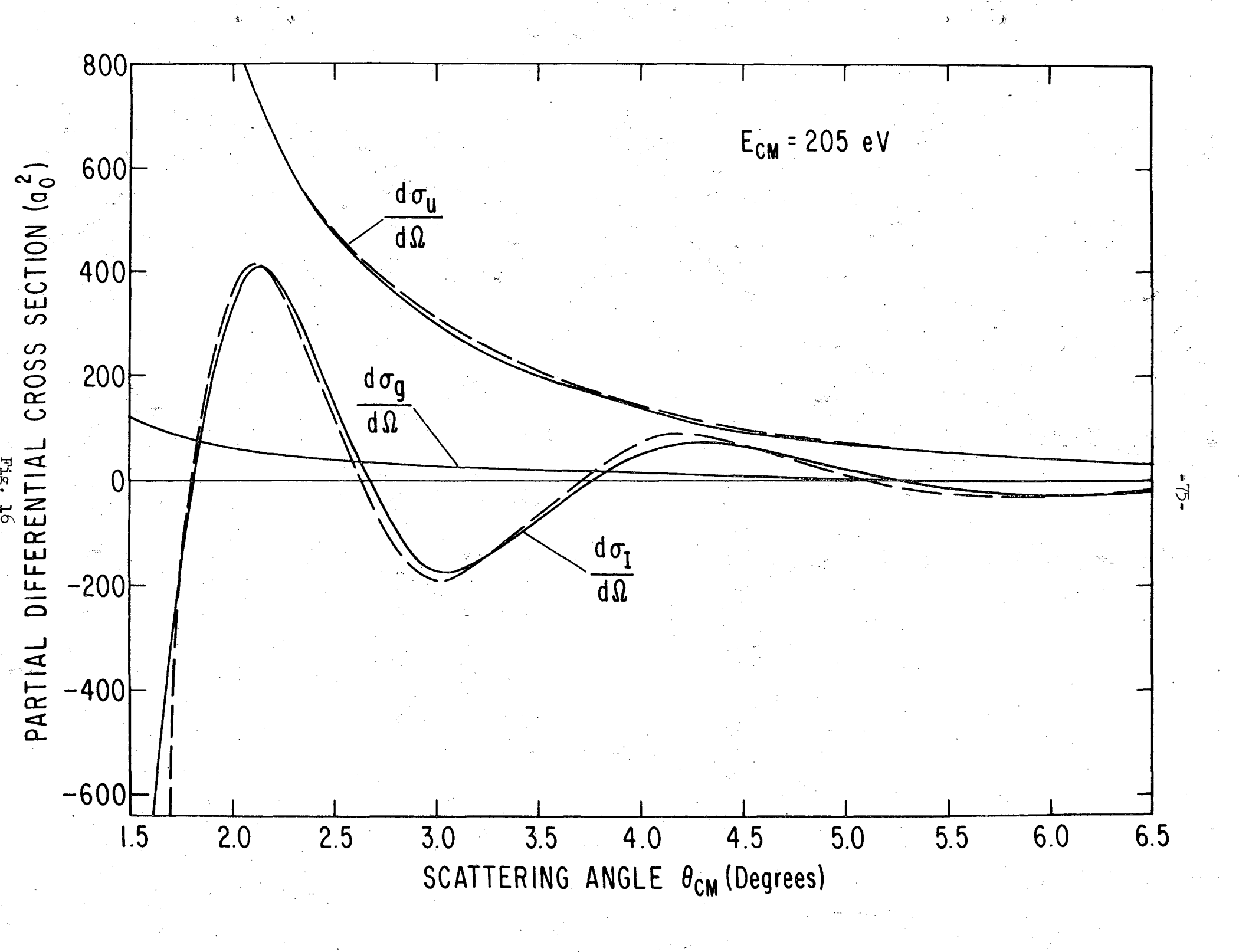
800
600
400
200
0
-200
-400
-600
1.5
2.0
2.5
3.0
3.5
4.0
4.5
5.0
5.5
6.0
6.5
E_{CM} = 205 eV
$\frac{d\sigma_u}{d\Omega}$
$\frac{d\sigma_g}{d\Omega}$
$\frac{d\sigma_I}{d\Omega}$
PARTIAL DIFFERENTIAL CROSS SECTION (a_0^2)
SCATTERING ANGLE θ_{CM} (Degrees)

Fig. 16

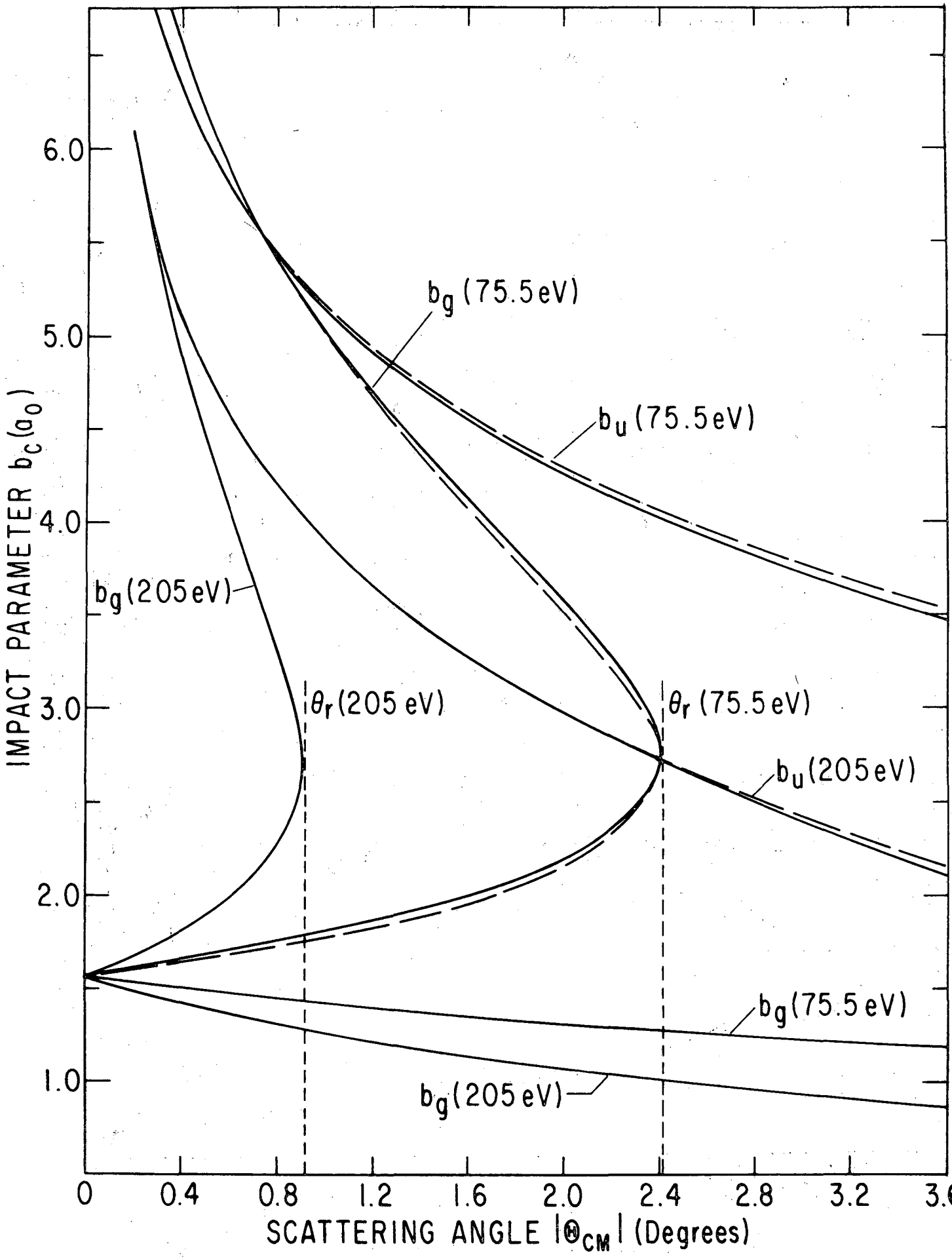
IMPACT PARAMETER $b_c(a_0)$
SCATTERING ANGLE $|\Theta_{CM}|$ (Degrees)
b_g (75.5eV)
b_u (75.5eV)
b_g(205eV)
θ_r(205 eV)
θ_r (75.5eV)
b_u(205eV)
b_g(75.5 eV)
b_g(205 eV)
6.0
5.0
4.0
3.0
2.0
1.0
0
0.4
0.8
1.2
1.6
2.0
2.4
2.8
3.2
3.6

Fig. 17

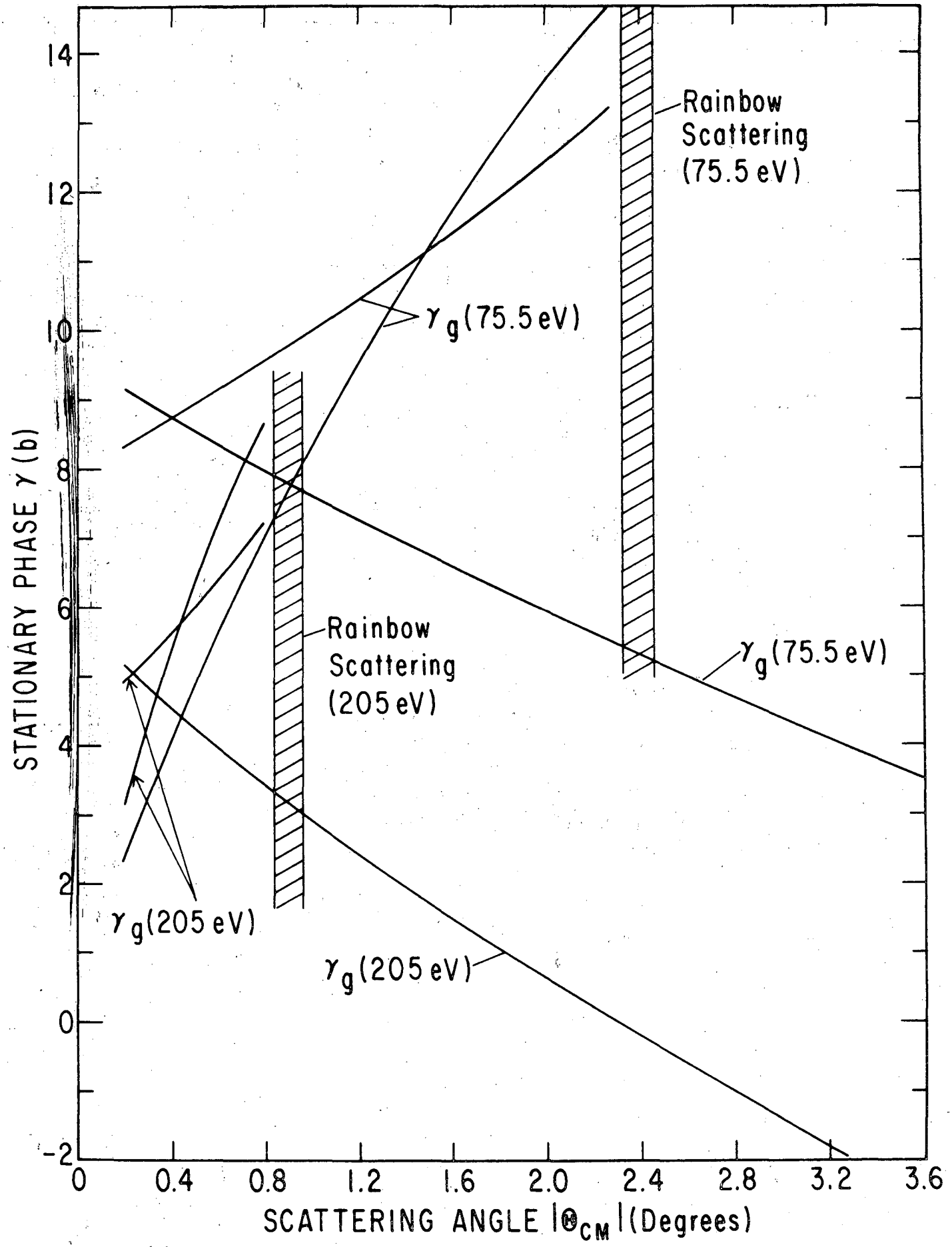
Rainbow
Scattering
(75.5 eV)
γ_g(75.5 eV)
Rainbow
Scattering
(205 eV)
γ_g(75.5 eV)
γ_g(205 eV)
γ_g(205 eV)
STATIONARY PHASE γ (b)
SCATTERING ANGLE $|\theta_{CM}|$ (Degrees)
14
12
10
8
6
4
2
0
-2
0
0.4
0.8
1.2
1.6
2.0
2.4
2.8
3.2
3.6

Fig. 18

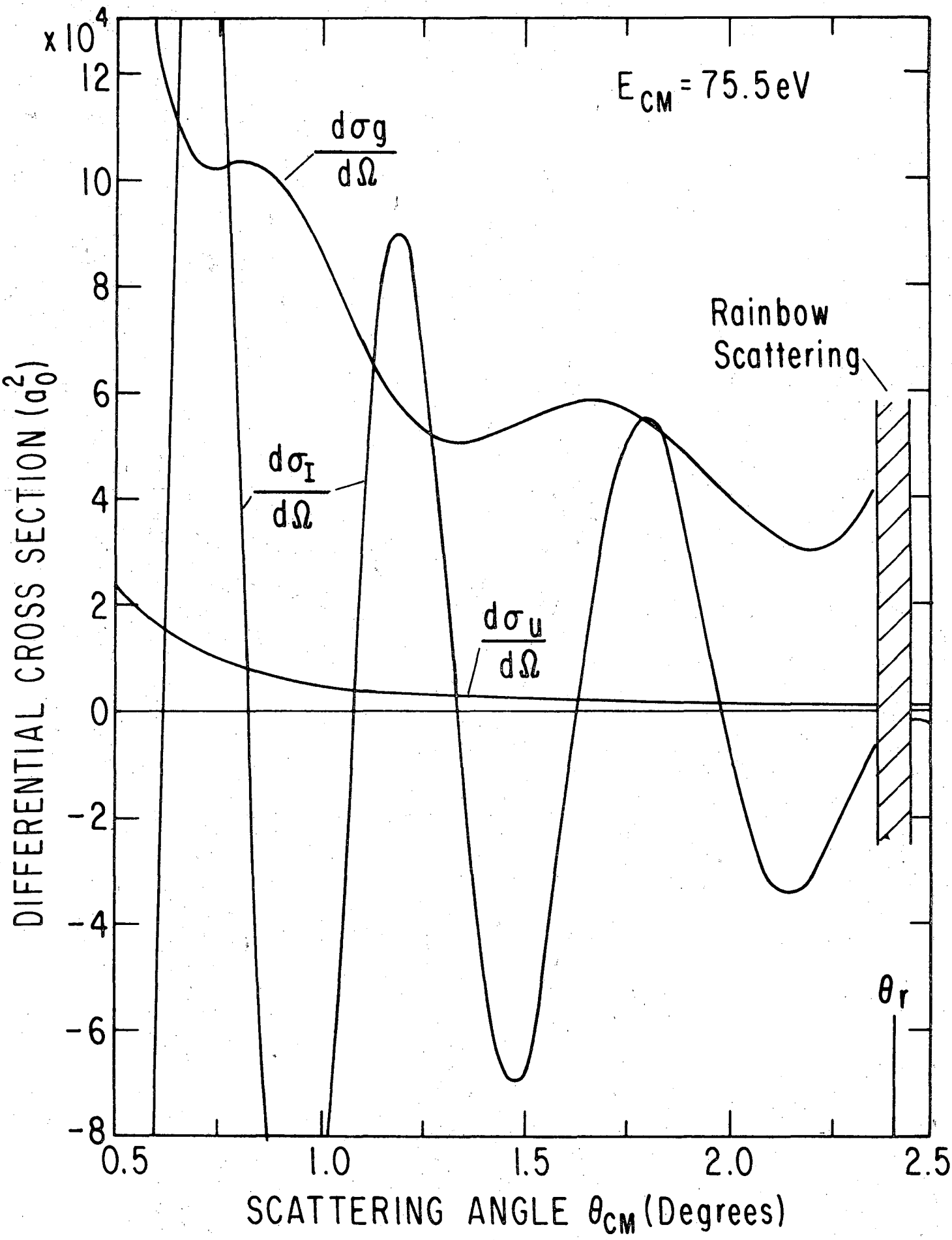
x 10^4
12
10
8
6
4
2
0
-2
-4
-6
-8
E_CM = 75.5eV
dσg/dΩ
dσI/dΩ
dσu/dΩ
Rainbow Scattering
θr
DIFFERENTIAL CROSS SECTION (a0^2)
0.5
1.0
1.5
2.0
2.5
SCATTERING ANGLE θCM (Degrees)

Fig. 19

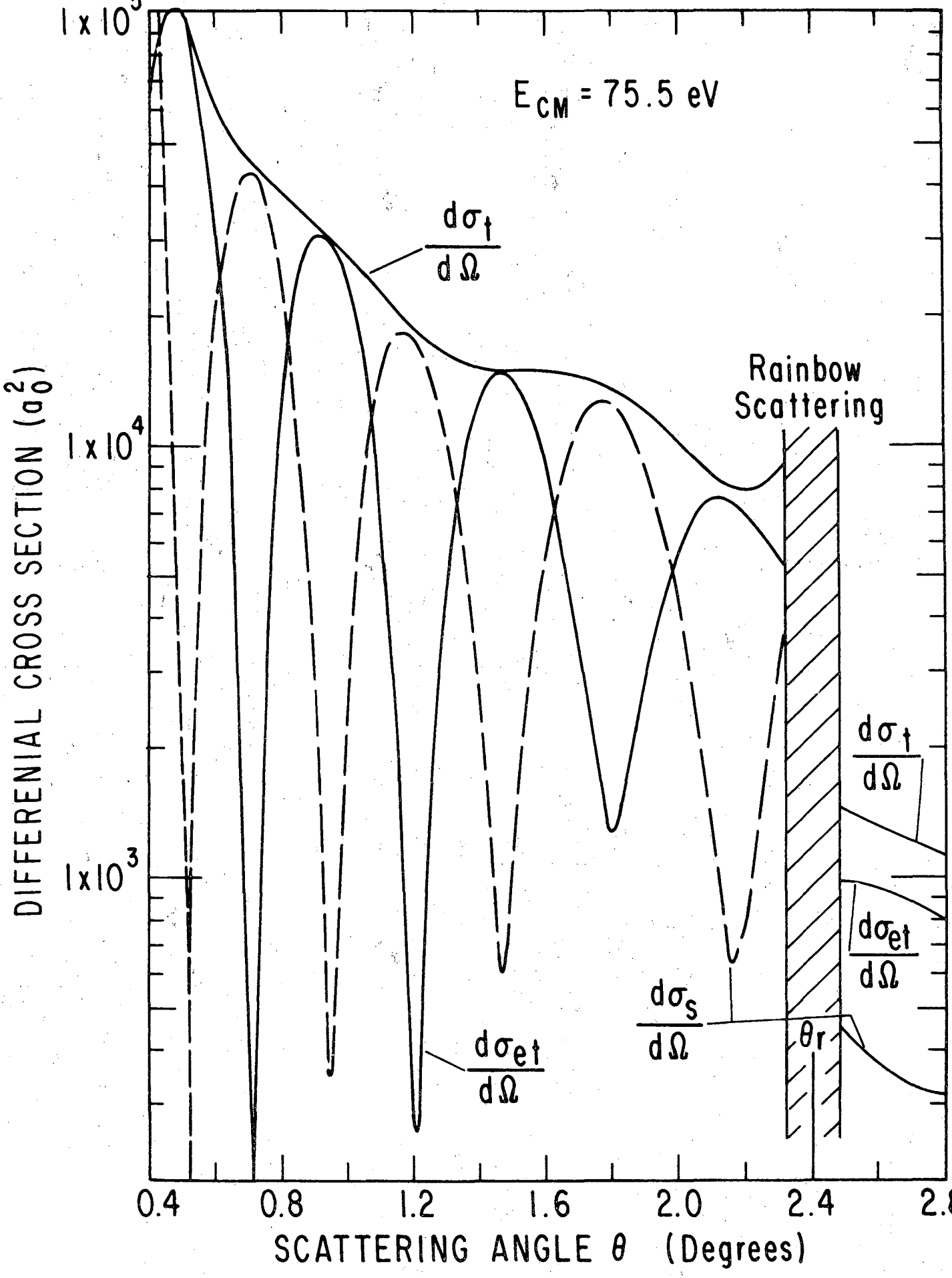
1 x 10^5
1 x 10^4
1 x 10^3
E_CM = 75.5 eV
dσ_t/dΩ
Rainbow Scattering
dσ_et/dΩ
dσ_s/dΩ
θr
DIFFERENIAL CROSS SECTION (a_0^2)
0.4
0.8
1.2
1.6
2.0
2.4
2.8
SCATTERING ANGLE θ (Degrees)

Fig. 20

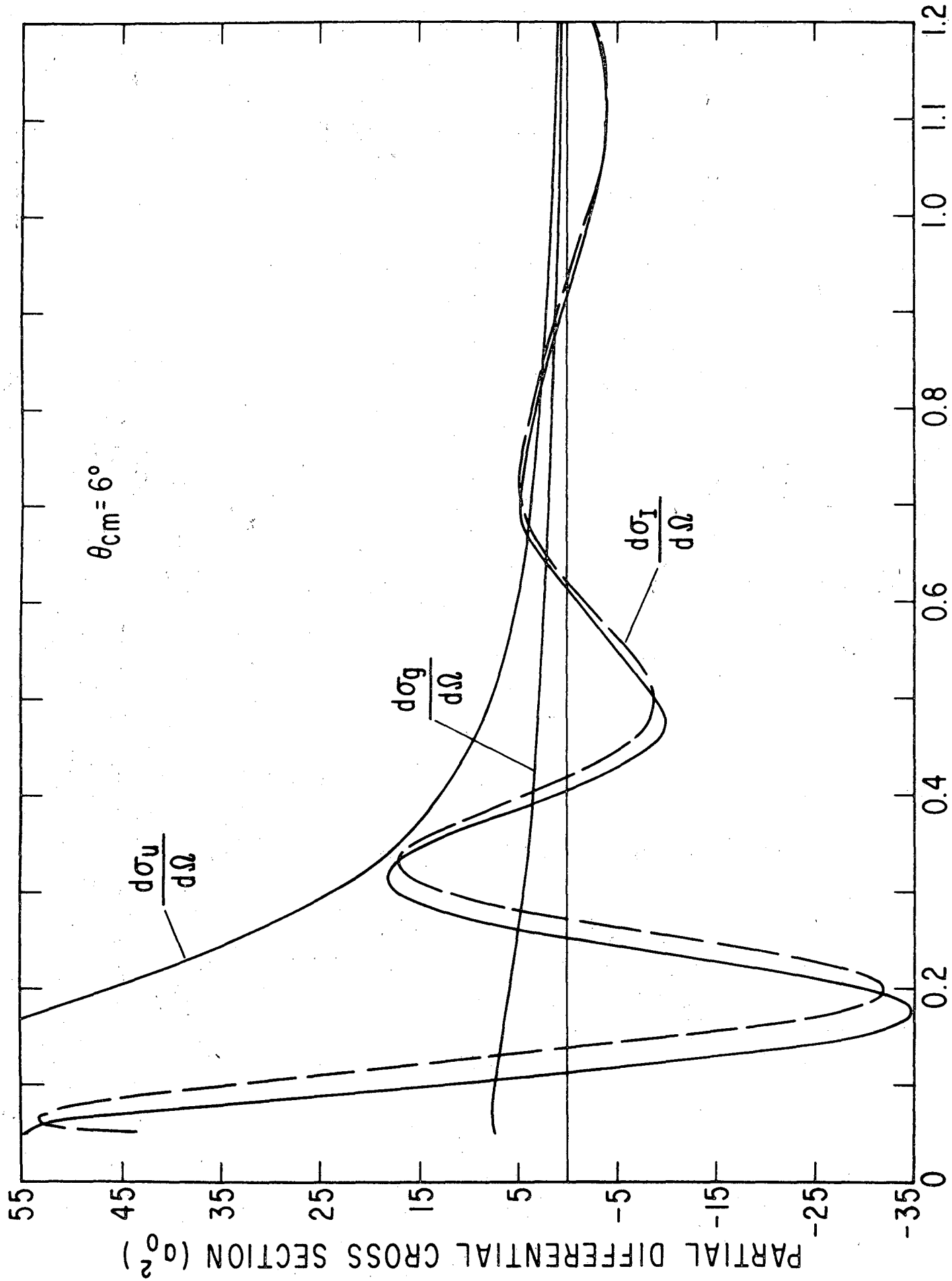
PARTIAL DIFFERENTIAL CROSS SECTION (a_0^2)
55
45
35
25
15
5
-5
-15
-25
-35
0
0.2
0.4
0.6
0.8
1.0
1.1
1.2
E_{cm} (KeV)
$\theta_{cm} = 6°$
$\frac{d\sigma_u}{d\Omega}$
$\frac{d\sigma_g}{d\Omega}$
$\frac{d\sigma_I}{d\Omega}$

Fig. 21

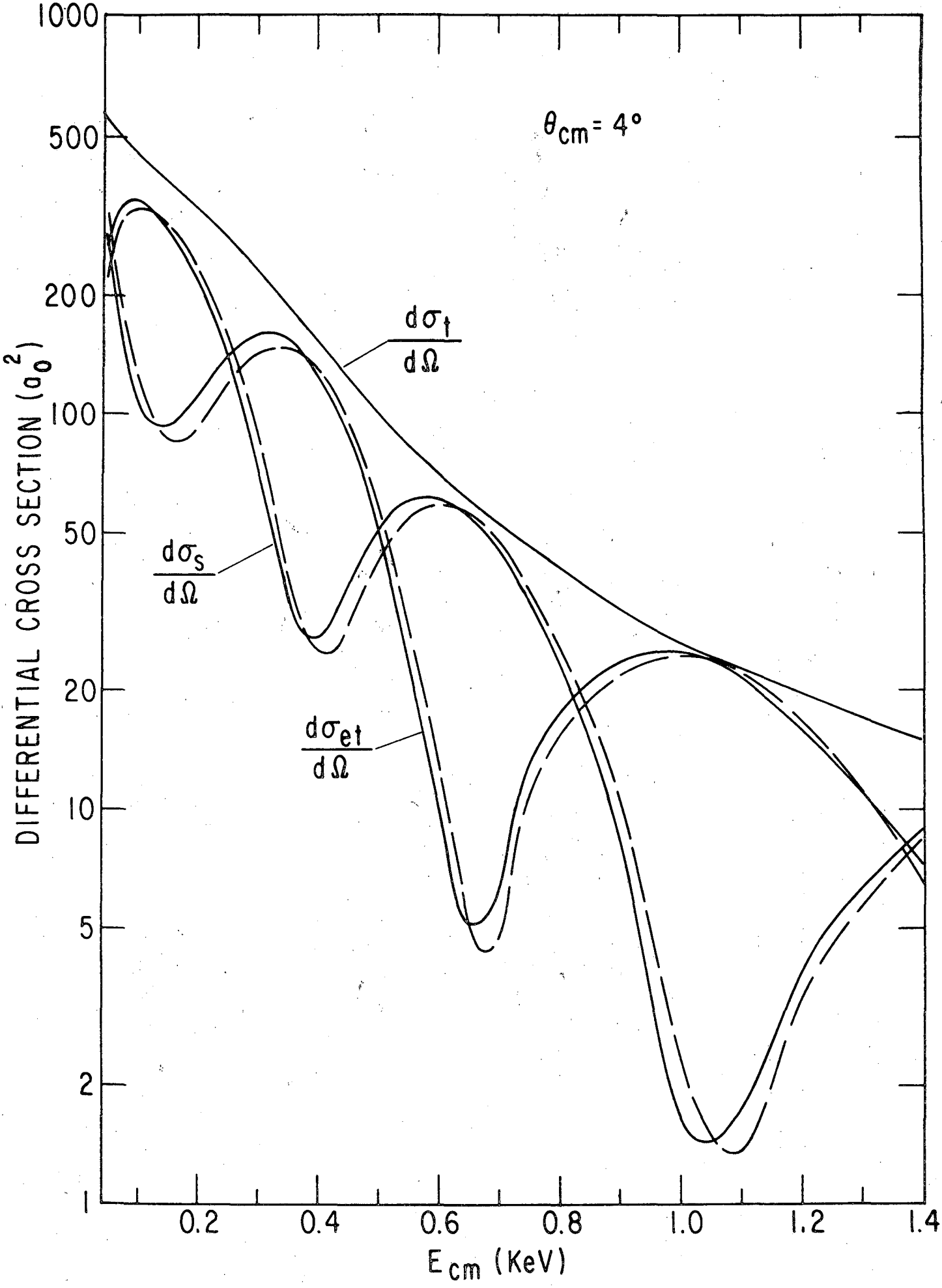
1000
500
200
100
50
20
10
5
2
1
0.2
0.4
0.6
0.8
1.0
1.2
1.4
$\theta_{cm} = 4°$
$\frac{d\sigma_t}{d\Omega}$
$\frac{d\sigma_s}{d\Omega}$
$\frac{d\sigma_{et}}{d\Omega}$
DIFFERENTIAL CROSS SECTION (a_o^2)
E_{cm} (KeV)

Fig. 22

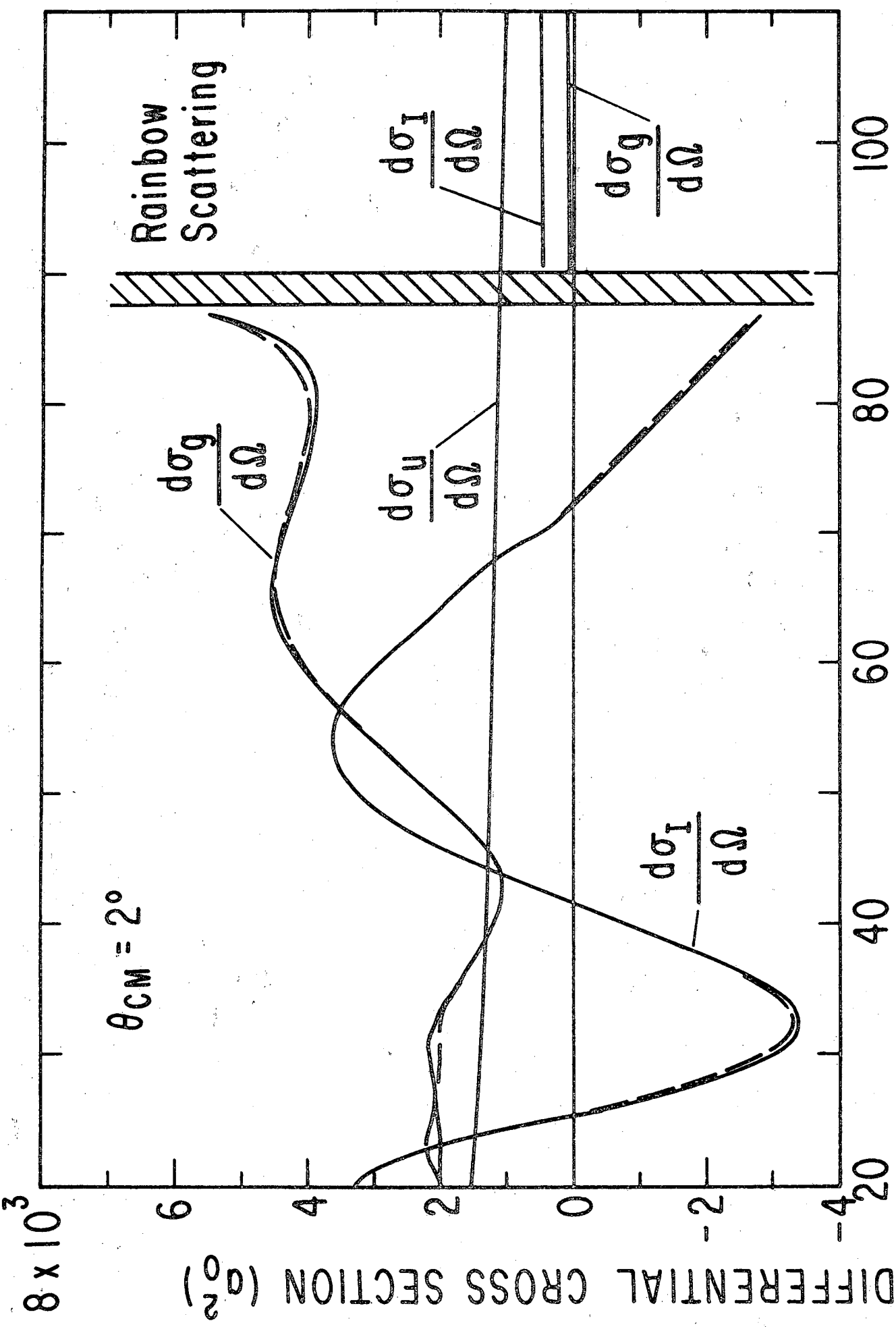
Rainbow Scattering
$\frac{d\sigma_I}{d\Omega}$
$\frac{d\sigma_g}{d\Omega}$
$\frac{d\sigma_g}{d\Omega}$
$\frac{d\sigma_u}{d\Omega}$
$\frac{d\sigma_I}{d\Omega}$
$\theta_{CM} = 2°$
8×10^3
DIFFERENTIAL CROSS SECTION (a_0^2)
6
4
2
0
-2
-4
20
40
60
80
100
E_{CM} (eV)

Fig. 23

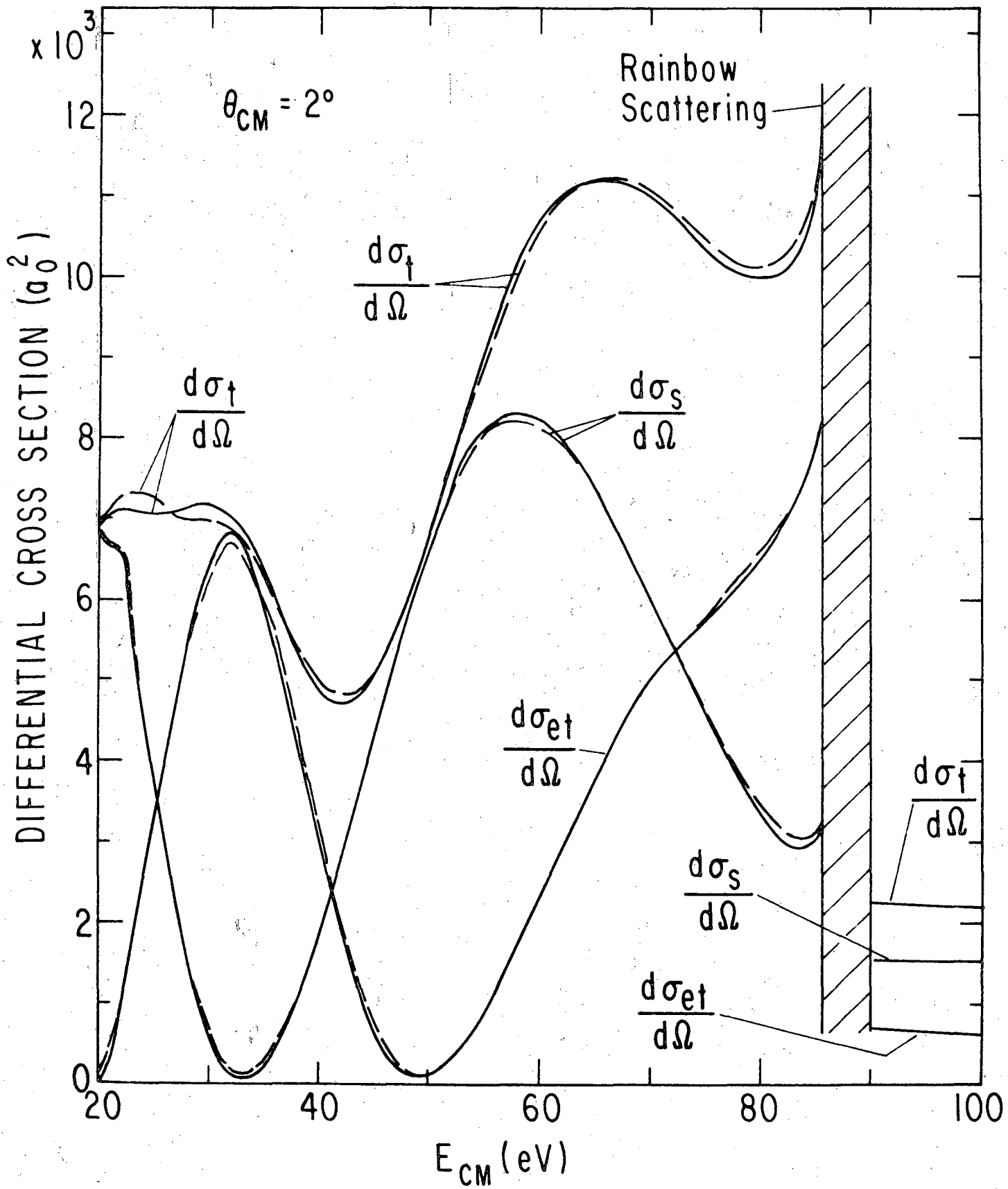
x 10^3
12
10
8
6
4
2
0
DIFFERENTIAL CROSS SECTION (a_0^2)
θ_CM = 2°
Rainbow Scattering
dσ_t/dΩ
dσ_t/dΩ
dσ_s/dΩ
dσ_et/dΩ
dσ_t/dΩ
dσ_s/dΩ
dσ_et/dΩ
20
40
60
80
100
E_CM (eV)

Fig. 24

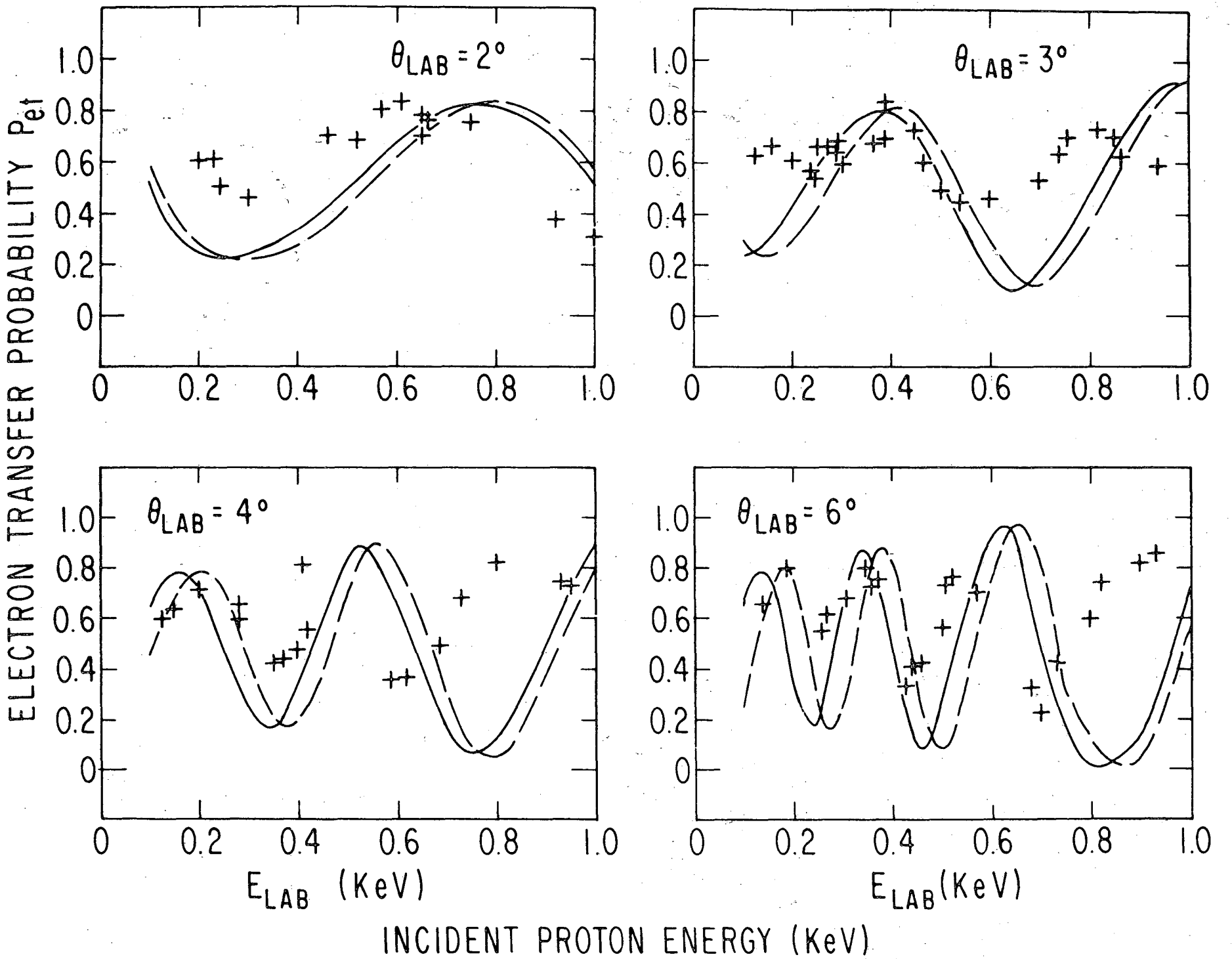
ELECTRON TRANSFER PROBABILITY P_{et}
$\theta_{LAB} = 2°$
$\theta_{LAB} = 3°$
$\theta_{LAB} = 4°$
$\theta_{LAB} = 6°$
1.0
0.8
0.6
0.4
0.2
0
0.2
0.4
0.6
0.8
1.0
E_{LAB} (KeV)
E_{LAB}(KeV)
INCIDENT PROTON ENERGY (KeV)

Fig. 25

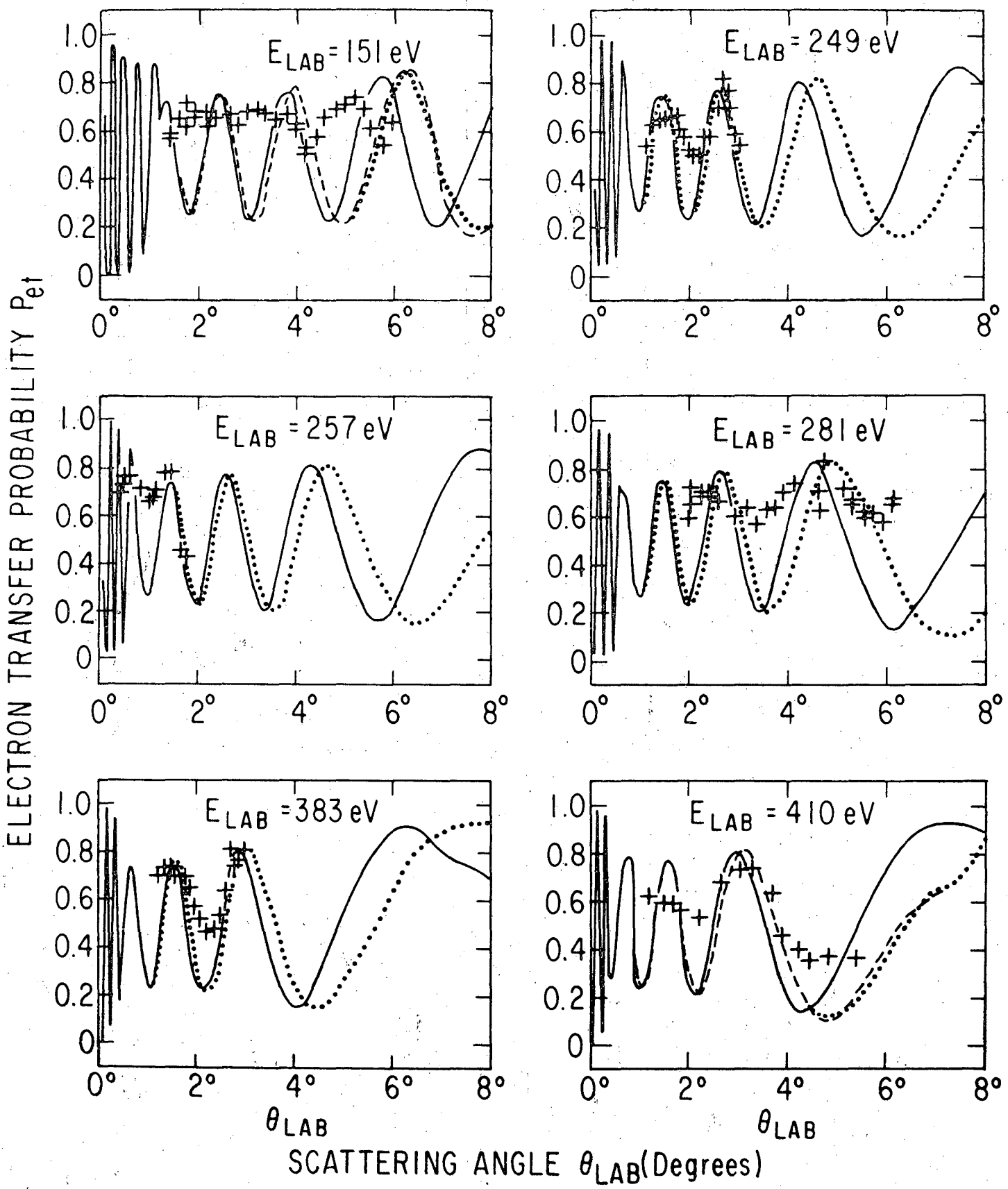
E_{LAB} = 151 eV
E_{LAB} = 249 eV
E_{LAB} = 257 eV
E_{LAB} = 281 eV
E_{LAB} = 383 eV
E_{LAB} = 410 eV
ELECTRON TRANSFER PROBABILITY P_{et}
1.0
0.8
0.6
0.4
0.2
0
0°
2°
4°
6°
8°
θ_{LAB}
SCATTERING ANGLE θ_{LAB}(Degrees)

Fig. 26

TECHNICAL INFORMATION DIVISION
LAWRENCE RADIATION LABORATORY
UNIVERSITY OF CALIFORNIA
BERKELEY, CALIFORNIA 94720